RT enzymes were expressed in *E. coli.* UTX81 and purified by the scheme described by Saitoh et al.[12] In vitro RT assays were conducted according to the previously described method with the following modifi cations.[13] Test compounds and 0.01 unit of recombinant HIV-1 RT (either wild type or mutant) were incubated in a reaction mixture (50 μL), containing 50 mM Tris–HCl (pH 8.4), 100 mM KCl, 10 mM $MgCl_2$, 0.1% Triton X-100, 2 mM dithiothreitol, 0.01 OD_{260} of poly(rC)/oligo(dG)$_{12-18}$, and 1 μCi of [1′,2′-^{3}H]dGTP (33 Ci/mmol) at 37 °C for 1 h. The reaction was stopped with 200 μL of 5% cold trichloroacetic acid. The precipitated materials were analyzed for radio activity using a scintillation counter (Aloka Co., Ltd., Tokyo, Japan).

5.2.2. Cells and viruses. MT-4 cells[14] and HIV-1$_{IIIB}$ were used for the anti-HIV-1 assays. MT-4 cells were grown and maintained in RPMI-1640 medium supplemented with 10% heat-inactivated fetal bovine serum (FBS), penicillin G (100 units/mL), and gentamicin (20 mg/mL). MT-4 cells and HIV-1$_{IIIB}$ were obtained from Rational Drug Design Laboratories (Fukushima, Japan).

5.2.3. Anti-HIV-1 assay. Determination of the antiviral activity of the test compounds against HIV-1$_{IIIB}$ replication was based on the inhibition of virus-induced cytopathicity in MT-4 cells. Briefly, MT-4 cells were suspended in culture medium at 1×10^5 cells/mL and infected with virus at a multiplicity of infection (MOI) of 0.02. Immediately after virus infection, the cell suspension (100 μL) was brought into each well of a flat-bottomed microtiter tray containing various concentrations of the test compounds. After a 5-day incubation at 37 °C, the number of viable cells was determined by the 3-(4,5-dimethylthiazol-2-yl)-2,5-diphenyltetrazolium bromide (MTT) method.[15] The HTS of our compound library was also performed using the MTT assay against HIV-1$_{IIIB\text{-}R}$.[14] The anti-HIV-1 activity and cytotoxicity of test compounds were expressed as EC_{50} and CC_{50}, respectively. EC_{50} is the concentration of a test compound that was able to achieve 50% protection of MT-4 cells from HIV-1 induced CPE. CC_{50} is the concentration of a test compound that reduced viable cell number by 50% in mock-infected cells. The therapeutic index (TI) is the ratio of CC_{50} to EC_{50}.

Acknowledgements

We wish to acknowledge helpful discussion with Dr. Susumu Igarashi. We also thank members of the Division of Analytical Research for performing instrumental analysis.

References and notes

1. Jonckheere, H.; Anné, J.; De Clercq, E. *Med. Res. Rev.* **2000**, *20*, 129.
2. Esnouf, R.; Ran, J.; Ross, C.; Jones, Y.; Stammers, D.; Stuart, D. *Nat. Struct. Biol.* **1995**, *2*, 303.
3. Richman, D. D.; Havlir, D.; Corbeil, J.; Looney, D.; Ignacio, C.; Spector, S. A.; Sullivan, J.; Cheeseman, S.; Barringer, K.; Pauletti, D. *J. Virol.* **1994**, *68*, 1660.
4. Bacheler, L. T. *Drug Resist. Updates* **1999**, *2*, 56.
5. Staszewski, S.; Morales-Ramirez, J.; Tashima, K. T.; Rachlis, A.; Skiest, D.; Stanford, J.; Stryker, R.; Johnson, P.; Labriola, D. F.; Farina, D.; Manion, D. J.; Ruiz, N. M. *N. Eng. J. Med.* **1999**, *341*, 1865.
6. Bacheler, L. T.; Anton, E. D.; Kudish, P.; Baker, D.; Bunville, J.; Krakowski, K.; Bolling, L.; Aujay, M.; Wang, X. V.; Ellis, D.; Becker, M. F.; Lasut, A. L.; George, H. J.; Spalding, D. R.; Hollis, G.; Abremski, K. *Antimicrob. Agents Chemother.* **2000**, *44*, 2475.
7. Masuda, N.; Yamamoto, O.; Fujii, M.; Ohgami, T.; Fujiyasu, J.; Kontani, T.; Moritomo, A.; Kageyama, S.; Ohta, M.; Orita, M.; Kurihara, H.; Koga, H.; Nakahara, H.; Inoue, H.; Hatta, T.; Suzuki, H.; Sudo, K.; Shimizu, Y.; Kodama, E.; Matsuoka, M.; Fujiwara, M.; Yokota, T.; Shigeta, S.; Baba, M. *Bioorg. Med. Chem.* **2004**, *12*, 6171–6182.
8. Saari, W. S.; Schwering, J. E. *J. Heterocycl. Chem.* **1986**, *23*, 1253.
9. Gerlach, U.; Wollmann, T. *Tetrahedron Lett.* **1992**, *33*, 5499.
10. Fuqiang, J. F.; Confalone, P. N. *Tetrahedron Lett.* **2000**, *41*, 3271.
11. Ouedraogo, R.; Becker, B.; Boverie, S.; Somers, F.; Antoine, M. H.; Pirotte, B.; Lebrun, P.; de Tullio, P. *Biol. Chem.* **2002**, *383*, 1759.
12. Saitoh, A.; Iwasaki, H.; Nakata, A.; Adachi, A.; Shinagawa, H. *Microbiol. Immunol.* **1990**, *34*, 509.
13. Baba, M.; De Clercq, E.; Tanaka, H.; Ubasawa, M.; Takashima, H.; Sekiya, K.; Nitta, I.; Umezu, K.; Nakashima, H.; Mori, S.; Shigeta, S.; Walker, R. T.; Miyasaka, T. *Proc. Natl. Acad. Sci. U.S.A.* **1991**, *88*, 2356.
14. Harada, S.; Koyanagi, Y.; Yamamoto, N. *Science* **1985**, *229*, 563.
15. Pauwels, R.; Balzarini, J.; Baba, M.; Snoeck, R.; Schols, D.; Herdewijn, P.; Desmyter, J.; De Clercq, E. *J. Virol. Methods* **1988**, *20*, 309.

ORGANIC LETTERS
2006
Vol. 8, No. 5
947–950

Potassium Carbonate-Promoted Stereospecific 5-*Endo-Trig* Cyclization of Unactivated Allenes in the Absence of Any Transition Metals

Hiroaki Ohno,*,† Yoichi Kadoh,‡ Nobutaka Fujii,† and Tetsuaki Tanaka*,‡

Graduate School of Pharmaceutical Sciences, Osaka University, 1-6 Yamadaoka, Suita, Osaka 565-0871, Japan, and Graduate School of Pharmaceutical Sciences, Kyoto University, Sakyo-ku, Kyoto 606-8501, Japan

hohno@pharm.kyoto-u.ac.jp; t-tanaka@phs.osaka-u.ac.jp

Received December 21, 2005

ABSTRACT

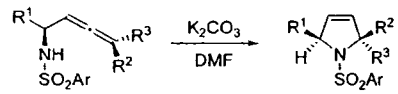

Formation of 3-pyrrolines from simple unactivated allenes bearing a protected amino group under basic conditions is described. Treatment of α-amino allenes with potassium carbonate in DMF under reflux in the absence of any transition-metal catalysts gave the corresponding 3-pyrrolines in good to excellent yields, by 5-*endo-trig* mode cycloisomerization. The reaction of internal allenes with an axial chirality afforded the corresponding 3-pyrrolines in a stereoselective manner.

Chiral 3-pyrrolines including 3,4-dehydroproline are known as useful synthetic intermediates for modified proline analogues,[1] conformationally restricted amino acid analogues,[2] antibiotic anisomycin,[3] and other related compounds.[4] Cycloisomerization of allenes through a 5-*endo-trig* mode is a powerful strategy for the construction of 3-pyrrolines[5] and other heterocycles such as dihydrofurans[6] and butenolides.[7] As shown in Scheme 1, this type of reaction

Scheme 1. Cycloisomerization of Allenes through 5-*Endo-Trig* Mode by Activation of Allenic Double Bond[a]

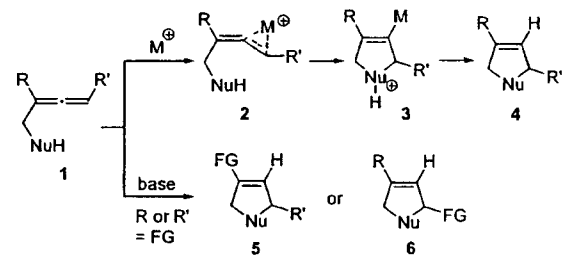

[a] FG = functional group.

generally proceeds through activation of the allenic moiety of **1** by coordination of transition metals such as Ag(I),[5-7] Pd(II),[8] Cu(I),[9] or Rh(I),[10] and subsequent attack by nitrogen or oxygen nucleophile onto the thus-activated allenic carbon of **2** leads to cyclized products **4** stereoselectively.[11] A recent contribution toward this area by Krause and Hashmi revealed that Au salts strongly catalyze the 5-*endo-trig* cycloisomerization of allenes **1** having a nitrogen or oxygen functional-

† Kyoto University.
‡ Osaka University.

(1) (a) Baldwin, J. E.; Field, R. A.; Lawrence, C. C.; Lee, V.; Robinson, J. K.; Schofield, C. J. *Tetrahedron Lett.* **1994**, *35*, 4649–4652. (b) Robinson, J. K.; Lee, V.; Claridge, T. D. W.; Baldwin, J. E.; Schofield, C. J. *Tetrahedron* **1998**, *54*, 981–996. (c) Ishii, K.; Ohno, H.; Takemoto, Y.; Ibuka, T. *Synlett* **1999**, 228–230. (d) Ishii, K.; Ohno, H.; Takemoto, Y.; Osawa, E.; Yamaoka, Y.; Fujii, N.; Ibuka, T. *J. Chem. Soc., Perkin Trans. 1* **1999**, 2155–2163.

(2) (a) Koskinen, A. M. P.; Rapoport, H. *J. Org. Chem.* **1989**, *54*, 1859–1866. (b) Chung, J. Y. L.; Wasicak, J. T.; Arnold, W. A.; May, C. S.; Nadzan, A. M.; Holladay, M. W. *J. Org. Chem.* **1990**, *55*, 270–275. (c) Holladay, M. W.; Lin, C. W.; May, C. S.; Garvey, D. S.; Witte, D. G.; Miller, T. R.; Wolfram, C. A. W.; Nadzan, A. M. *J. Med. Chem.* **1991**, *34*, 455–457.

(3) Jegham, S.; Das, B. C. *Tetrahedron Lett.* **1988**, *29*, 4419–4422.

(4) (a) Burley, I.; Hewson, A. T. *Tetrahedron Lett.* **1994**, *35*, 7099–7102. (b) Horikawa, M.; Shirahama, H. *Synlett* **1996**, 95–96. (c) Sibi, M. P.; Christensen, J. W. *Tetrahedron Lett.* **1995**, *36*, 6213–6216.

10.1021/ol053094w CCC: $33.50
Published on Web 02/07/2006

ity.[12,13] In contrast, only limited examples of the *endo*-mode cycloisomerization under basic conditions in the absence of any transition metals are reported to date, which used preactivated allenes **1** (R or R′ = functional group) such as methoxy allenes,[14,15] fluorinated allenes,[16] or allenyl sulfones and related compounds,[17] leading to functionalized cyclized products **5** or **6**.

As a part of our ongoing program directed toward economical and environmentally friendly cyclization of allenic compounds,[18−20] we investigated cycloisomerization of amino allenes without using any transition-metal catalysts. Herein, we describe K_2CO_3-mediated stereospecific cycloisomerization of α-amino allenes, which is the first example of base-induced 5-*endo*-*trig* mode cycloisomerization of simple unactivated allenes in the absence of any activating reagents toward the allenic π-bond.

We prepared α-amino allene **7** according to our reported procedure through the diethylzinc-mediated reductive synthesis of amino allenes catalyzed by palladium(0),[21] starting from L-valine. The choice of Mts as a protecting group was based primarily on its ease of deprotection.[22] First, cycloisomerization of **7** under various basic conditions (NaH/DMF, *t*-BuOK/DMF, or *n*-BuLi/THF, etc.) was investigated, and we found that treatment of **7** with K_2CO_3 in a polar solvent in high temperature afforded the desired cycloisomerized product **8** (Table 1). Among the solvents investigated (Table 1, entries 1−4), DMF has proven to be the solvent of choice for the desired transformation, leading to 3-pyrroline **8** in 84% yield (Table 1, entry 4). A catalytic amount of K_2CO_3 did promote the cycloisomerization (Table 1, entries 5 and 6) but required prolonged reaction time: the cyclization with 0.1 equiv of K_2CO_3 for 120 h yielded **8** (47%) with the recovered starting material (7%). Structure of **8** was unambiguously confirmed by comparison with the authentic sample.[23]

Table 1. Optimization of Reaction Conditions

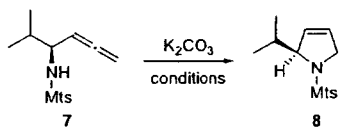

entry	K_2CO_3 (equiv)	solvent	T (°C)	reaction time (h)	yield[a] (%)
1	1.0	DMSO	180	3	61
2	1.0	DMI	180	1	75
3	1.0	NMP	180	3	80
4	1.0	DMF	reflux	6	84
5	0.5	DMF	reflux	24	71
6	0.1	DMF	reflux	120	47

[a] Isolated yields. Mts = 2,4,6-trimethylphenylsulfonyl.

Next, K_2CO_3-promoted cyclization of other terminal allenes **9**−**12** was investigated (Table 2). The reaction of

(5) (a) Claesson, A.; Sahlberg, C.; Luthman, K. *Acta Chem. Scand.* **1979**, *B33*, 309−310. (b) Lathbury, D.; Gallagher, T. *J. Chem. Soc., Chem. Commun.* **1986**, 114−115. (c) Kinsman, R.; Lathbury, D.; Vernon, P.; Gallapher, T. *J. Chem. Soc., Chem. Commun.* **1987**, 243−244. (d) Prasad, J. S.; Liebeskind, L. S. *Tetrahedron Lett.* **1988**, *29*, 4253−4256. (e) Fox, D. N. A.; Lathbury, D.; Mahon, M. F.; Molloy, K. C.; Gallagher, T. *J. Chem. Soc., Chem. Commun.* **1989**, 1073−1075. (f) Ohno, H.; Toda, A.; Miwa, Y.; Taga, T.; Osawa, E.; Yamaoka, Y.; Fujii, N.; Ibuka, T. *J. Org. Chem.* **1999**, *64*, 2992−2993. (g) Dieter, R. K.; Yu, H. *Org. Lett.* **2001**, *3*, 3855−3858.

(6) (a) Olsson, L.-I.; Claesson, A. *Synthesis* **1979**, 743−745. (b) Fujisawa, T.; Machata, E.; Kohama, H.; Sato, T. *Chem. Lett.* **1985**, 1457−1458. (c) Nikam, S. S.; Chu, K.-H.; Wang, K. K. *J. Org. Chem.* **1986**, *51*, 745−747. (d) Marshall, J. A.; Wang, X.-J. *J. Org. Chem.* **1990**, *55*, 2995−2996. (e) VanBrunt, M. P.; Standaert, R. F. *Org. Lett.* **2000**, *2*, 705−708. (f) Lepage, O.; Kattnig, E.; Fürstner, A. *J. Am. Chem. Soc.* **2004**, *126*, 15970−15971.

(7) (a) Gill, G. B.; Idris, M. S. H. *Tetrahedron Lett.* **1985**, *26*, 4811−4814. (b) Marshall, J. A.; Wolf, M. A.; Wallace, E. M. *J. Org. Chem.* **1997**, *62*, 367−371. (c) Yoneda, E.; Kaneko, T.; Zhang, S.-W.; Onitsuka, K.; Takahashi, S. *Org. Lett.* **2000**, *2*, 441−443.

(8) Hashmi, A. S. K.; Ruppert, T. L.; Knöfel, T.; Bats, J. W. *J. Org. Chem.* **1997**, *62*, 7295−7304.

(9) (a) Ma, S.; Yu, Z.; Wu, S. *Tetrahedron* **2001**, *57*, 1585−1588. (b) Kel'in, A. V.; Gevorgyan, V. *J. Org. Chem.* **2002**, *67*, 95−98.

(10) Marshall, J. A.; Robinson, E. D. *J. Org. Chem.* **1990**, *55*, 3450−3451.

(11) For a related cycloisomerizations, see: (a) Arseniyadis, S.; Sartoretti, J. *Tetrahedron Lett.* **1985**, *26*, 729−732. (b) Grimaldi, J.; Cormons, A. *Tetrahedron Lett.* **1986**, *27*, 5089−5090. (c) Meguro, M.; Yamamoto, Y. *Tetrahedron Lett.* **1998**, *39*, 5421−5424. (d) Arredondo, V. M.; Tian, S.; McDonald, F. E.; Marks, T. J. *J. Am. Chem. Soc.* **1999**, *121*, 3633−3639. (e) Ha, J. D.; Cha, J. K. *J. Am. Chem. Soc.* **1999**, *121*, 10012−10020.

(12) (a) Hashmi, A. S. K.; Schwarz, L.; Choi, J.-H.; Frost, T. M. *Angew. Chem., Int. Ed.* **2000**, *39*, 2285−2288. (b) Hoffman-Röder, A.; Krause, N. *Org. Lett.* **2001**, *3*, 2537−2538. (c) Morita, N.; Krause, N. *Org. Lett.* **2004**, *6*, 4121−4123. (d) Lee, P. H.; Kim, H.; Lee, K.; Kim, M.; Noh, K.; Kim, H.; Seomoon, D. *Angew. Chem., Int. Ed.* **2005**, *44*, 1840−1843.

(13) For HCl gas-mediated cyclization, see: Krause, N.; Laux, M.; Hoffmann-Röder, A. *Tetrahedron Lett.* **2000**, *41*, 9613−9616.

(14) (a) Gange, D.; Magnus, P. *J. Am. Chem. Soc.* **1978**, *100*, 7746−7747. (b) Hormuth, S.; Reissig, H.-U. *J. Org. Chem.* **1994**, *59*, 67−73. (c) Breuil-Desvergnes, V.; Compain, P.; Vatèle, J.-M.; Goré, J. *Tetrahedron Lett.* **1999**, *40*, 5009−5012. (d) Amombo, M. O.; Hausherr, A.; Reissig, H.-U. *Synlett* **1999**, 1871−1874. (e) Breuil-Desvergnes, V.; Goré, J. *Tetrahedron* **2001**, *57*, 1939−1950. (f) Flögel, O.; Amombo, M. G. O.; Reissig, H.-U.; Zahn, G.; Brüdgam, I.; Hartl, H. *Chem. Eur. J.* **2003**, *9*, 1405−1415.

(15) A methoxy group on the allenic carbon promotes single electron transfer from the dimsylate anion to give radical anion intermediate: see: Magnus, P.; Albaugh-Robertson, P. *J. Chem. Soc., Chem. Commun.* **1984**, 804−806.

(16) (a) Wang, Z.; Hammond, G. B. *J. Org. Chem.* **2000**, *65*, 6547−6552. (b) Lan, Y.; Hammond, G. B. *Org. Lett.* **2002**, *4*, 2437−2439.

(17) (a) Mukai, C.; Yamashita, H.; Hanaoka, M. *Org. Lett.* **2001**, *3*, 3385−3387. (b) Mukai, C.; Ohta, M.; Yamashita, H.; Kitagaki, S. *J. Org. Chem.* **2004**, *69*, 6867−6873. See also: (c) Pravia, K.; White, R.; Fodda, R.; Maynard, D. F. *J. Org. Chem.* **1996**, *61*, 6031−6032.

(18) For our recent contribution on [2 + 2] cycloisomerization of allenenes or allenynes without using any reagents or catalysts, see: Ohno, H.; Mizutani, T.; Kadoh, Y.; Miyamura, K.; Tanaka, T. *Angew. Chem., Int. Ed.* **2005**, *44*, 5113−5115.

(19) For our recent contribution on tandem cyclization of allenenes and related compounds, see: (a) Ohno, H.; Miyamura, K.; Takeoka, Y.; Tanaka, T. *Angew. Chem., Int. Ed.* **2003**, *42*, 2647−2650. (b) Ohno, H.; Miyamura, K.; Mizutani, T.; Kadoh, Y.; Takeoka, Y.; Hamaguchi, H.; Tanaka, T. *Chem. Eur. J.* **2005**, *11*, 3728−3741. (c) Ohno, H.; Yamamoto, M.; Iuchi, M.; Tanaka, T. *Angew. Chem., Int. Ed.* **2005**, *44*, 5103−5106.

(20) For our recent contribution on tandem reaction of bromoallenes, see: (a) Ohno, H.; Hamaguchi, H.; Ohata, M.; Tanaka, T. *Angew. Chem., Int. Ed.* **2003**, *42*, 1749−1753. (b) Ohno, H.; Hamaguchi, H.; Ohata, M.; Kosaka, S.; Tanaka, T. *Heterocycles* **2003**, *61*, 65−68. (c) Ohno, H.; Hamaguchi, H.; Ohata, M.; Kosaka, S.; Tanaka, T. *J. Am. Chem. Soc.* **2004**, *126*, 8744−8754. (d) Hamaguchi, H.; Kosaka, S.; Ohno, H.; Tanaka, T. *Angew. Chem., Int. Ed.* **2005**, *44*, 1513−1517. (e) Ohno, H. *Chem. Pharm. Bull.* **2005**, *53*, 1211−1226. (f) Ohno, H. *Yakugaku Zasshi* **2005**, *125*, 899−925.

(21) (a) Ohno, H.; Toda, A.; Oishi, S.; Tanaka, T.; Takemoto, Y.; Fujii, N.; Ibuka, T. *Tetrahedron Lett.* **2000**, *41*, 5131−5134. (b) Ohno, H.; Miyamura, K.; Tanaka, T.; Oishi, S.; Toda, A.; Takemoto, Y.; Fujii, N.; Ibuka, T. *J. Org. Chem.* **2002**, *67*, 1359−1367.

(22) Unfortunately, treatment of *N*-Boc derivatives under the K_2CO_3-mediated cyclization conditions gave a mixture of unidentified products.

(23) Cyclized products **8**, **14**, and the enantiomers of **21** and **22** were previously prepared by our group, see refs 1c,d and 5f.

Table 2. K_2CO_3-Promoted Cycloisomerization of Terminal Allenes[a]

entry	substrate	time (h)	product	yield (%)[b]
1	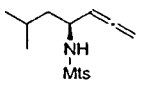 **9**	120	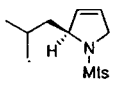 **13**	61
2	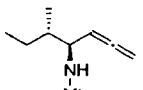 **10**	72	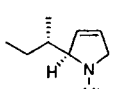 **14**	60
3	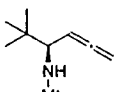 **11**	20	 **15**	78
4	 **12**	1	 **16**	77

[a] All reactions were carried out in the presence of K_2CO_3 (1 equiv) in DMF under reflux. [b] Isolated yields.

Table 3. K_2CO_3–Promoted Cycloisomerization of Internal Allenes[a]

entry	substrate	time (h)	product	yield (%)[b]
1	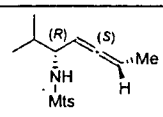 **17**	18	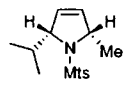 **21**	80
2	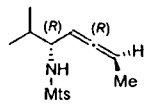 **18**	102	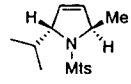 **22**	83
3	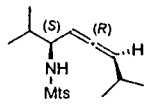 **19**	24	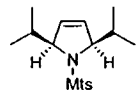 **23**	87
4	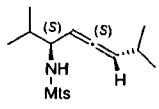 **20**	312	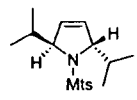 **24**	75

[a] All reactions were carried out in the presence of K_2CO_3 (1 equiv) in DMF under reflux. [b] Isolated yields.

amino allene **9** or **10** having an isobutyl group or a *sec*-butyl group, respectively, at the α-position of the allenic moiety with K_2CO_3 in DMF under reflux yielded the desired cyclized products **13** and **14** in 61% and 60% yields, respectively (Table 2, entries 1 and 2). Interestingly, both the allenes **11** with a bulky *tert*-butyl group and **12** without the α-substituent gave 3-pyrrolines **15** and **16** in slightly improved yields (77–78%). The required reaction time for this transformation is highly dependent on the α-substituent (1–120 h). Among the terminal allenes **7** and **9**–**12**, the α-unsubstituted amino allenes **12** showed the highest reactivity toward the K_2CO_3-mediated cycloisomerization: the reaction was completed within 1 h under the standard reaction conditions.

Then, the cycloisomerization of diastereomerically pure internal allenes bearing an α-amino group was investigated. The requisite chiral internal allenes **17**–**20** were easily prepared by organocopper-mediated stereospecific ring-opening reaction of 2-ethynylaziridines derived from L- or D-amino acids.[24] The results of the cycloisomerization reaction are summarized in Table 3. We were pleased to find that the reaction of all the internal allenes yielded 2,5-disubstituted 3-pyrrolines in a stereospecific manner and in good yields (75–87%). The reaction of (*R*,a*S*)- and (*S*,a*R*)-allenes **17** and **19**, respectively, completed within 24 h to give the 2,5-*cis*-3-pyrrolines **21** and **23**. In contrast, the reactivity of (*R*,a*R*)- and (*S*,a*S*)-allenes **18** and **20** was relatively low: the 2,5-*trans*-3-pyrrolines **22** and **24**, the latter having C_2-symmetry, were obtained after prolonged reaction time (102–312 h) but in good yields.[25] The relative configuration of the cyclized products **21** and **22** was determined by comparison with the authentic samples.[23]

It should be clearly noted that the internal allene **19** bearing an isopropyl group on the allenic carbon was completely inert toward the well-established silver(I)-mediated cyclization (Scheme 2). This result can be attributed to the steric

Scheme 2

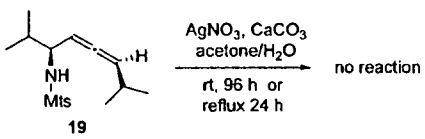

crowding of the allenic moiety that inhibits access or coordination of silver to the allenic double bond. In contrast, K_2CO_3-induced reaction of **19** afforded the sterically congested *meso*-2,5-disubstituted 3-pyrroline **23** in 87% yield (Table 3, entry 3), presumably because these conditions activate the nitrogen atom of the amino allene **19**.

In conclusion, we have first demonstrated that cycloisomerization of unactivated allenes having a sulfonamide group can be promoted under simple basic conditions using

(24) (a) Ohno, H.; Toda, A.; Miwa, Y.; Taga, T.; Fujii, N.; Ibuka, T. *Tetrahedron Lett.* **1999**, *40*, 349–352. (b) Ohno, H.; Toda, A.; Fujii, N.; Takemoto, Y.; Tanaka, T.; Ibuka, T. *Tetrahedron* **2000**, *56*, 2811–2820.

(25) The lower reactivity of **18** and **20** will be an influence of the Mts group: the aryl group of Mts will direct the opposite side to the isopropyl group at the α position, which may cause an unfavorable steric interaction to the alkyl group on the allenyl carbon on cyclization. However, the exact reason for their lower reactivity is unclear.

K_2CO_3 in DMF. The present transformation is economical and applicable to the synthesis of a wide variety of 3-pyrrolines including highly congested ones. The scope and limitation of the reaction, as well as further transformation to complex nitrogen heterocycles, are currently under investigation.

Acknowledgment. This work was supported by a Grant-in-Aid for Encouragement of Young Scientists from the Ministry of Education, Culture, Sports, Science and Technology of Japan and Mitsubishi Chemical Corporation Fund. which are gratefully acknowledged.

Supporting Information Available: Representative experimental procedure, as well as ^1H NMR spectra for the novel cyclized products. This material is available free of charge via the Internet at http://pubs.acs.org.

OL053094W

ORGANIC LETTERS
2006
Vol. 8, No. 4
613–616

Unequivocal Synthesis of (*Z*)-Alkene and (*E*)-Fluoroalkene Dipeptide Isosteres To Probe Structural Requirements of the Peptide Transporter PEPT1

Ayumu Niida,[†] Kenji Tomita,[†] Makiko Mizumoto,[†] Hiroaki Tanigaki,[†] Tomohiro Terada,[‡] Shinya Oishi,[†] Akira Otaka,[†,§] Ken-ichi Inui,[‡] and Nobutaka Fujii*,[†]

Graduate School of Pharmaceutical Sciences, Kyoto University, Sakyo-ku, Kyoto 606-8501, Japan, Department of Pharmacy, Kyoto University Hospital, Sakyo-ku, Kyoto 606-8507, Japan, and Graduate School of Pharmaceutical Sciences, The University of Tokushima, Tokushima 770-8505, Japan

nfujii@pharm.kyoto-u.ac.jp

Received November 17, 2005

ABSTRACT

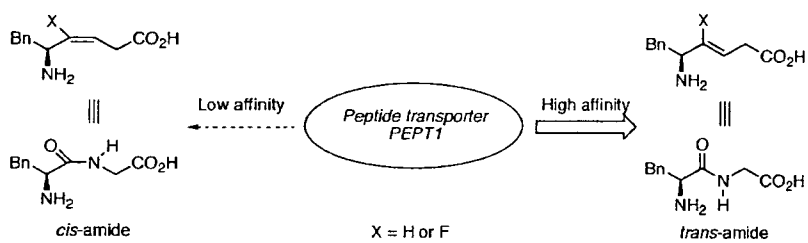

Described is a novel synthetic route for dipeptide isosteres containing (*Z*)-alkene and (*E*)-fluoroalkene units as *cis*-amide bond equivalents via organocopper-mediated reduction of γ-acetoxy- or γ,γ-difluoro-α,β-unsaturated-δ-lactams. The synthesized isosteres were evaluated in terms of their affinities for the peptide transporter PEPT1. *trans*-Amide isosteres tended to possess higher affinities for PEPT1 as compared to the corresponding *cis*-amide bond equivalents.

In postgenomic drug discovery research, the rapid elucidation of structural requirements of the ligands for newly identified drug targets (e.g., GPCRs, enzymes, transporters, etc.) is strongly needed in the arena of medicinal chemistry.[1] Many protein drug targets interact with proteinic or peptidic ligands. Therefore, development of peptidomimetic small molecules is important for investigating criteria for the mutual molecular recognition.[2] Alkene-type dipeptide isosteres represent potential amide bond mimetics (Figure 1).[3] Fluoroalkene dipeptide isosteres were designed as electrostatically favorable mimetics as compared to simple alkene isosteres.[4] These isosteres have structural similarities with the parent peptides

[†] Graduate School of Pharmaceutical Sciences, Kyoto University.
[‡] Kyoto University Hospital.
[§] The University of Tokushima.

(1) (a) Drews, J. *Science* **2000**, *287*, 1960. (b) Klabunde, T.; Hessler, G. *ChemBioChem* **2002**, *3*, 928. (c) Tyndall, J. D. A.; Pfeiffer, B.; Abbenante, G., Fairlie, D. P. *Chem. Rev.* **2005**, *105*, 793.

(2) (a) Burgess, K. *Acc. Chem. Res.* **2001**, 34, 826. (b) Bursavich M. G.; Rich, D. H. *J. Med. Chem.* **2002**, *45*, 541. (c) Hruby, V. J. *J. Med Chem.* **2003**, *46*, 4215.

(3) (a) Oishi, S.; Kamano, T.; Niida, A.; Odagaki, Y.; Hamanaka, N.; Yamamoto, M.; Ajito, K.; Tamamura, H.; Otaka, A.; Fujii, N. *J. Org. Chem.* **2002**, *67*, 6162. (b) Wipf, P.; Xiao, J. *Org. Lett.* **2005**, *7*, 103. (c) Xiao, J.; Weisblum, B.; Wipf, P. *J. Am. Chem. Soc.* **2005**, *127*, 5742.

(4) (a) Abraham, R. J.; Ellison, S. L. R.; Schonholzer, P.; Thomas, W. A. *Tetrahedron* **1986**, *42*, 2101. (b) Allmendinger, T.; Furet, P.; Hungerbühler, E.; *Tetrahedron Lett.* **1990**, *31*, 7297. (c) Allmendinger, T.; Furet, P.; Hungerbühler, E.; *Tetrahedron Lett.* **1990**, *31*, 7301. (d) Otaka, A.; Watanabe, J.; Yukimasa, A.; Sasaki, Y.; Watanabe, H.; Kinoshita, T.; Oishi, S.; Tamamura, H.; Fujii, N. *J. Org. Chem.* **2004**, *69*, 1634. (e) V. d. Veken, P.; Senten, K.; Kertèsz, I.; D. Meester, I.; Lambeir, A.-M.; Maes, M.-B.; Scharpè, S.; Haemers, A.; Augustyns, K. *J. Med. Chem.* **2005**, *48*, 1768. (f) Nakamura, Y.; Okada, M.; Sato, A.; Horikawa, H.; Koura, M.; Saito, A.; Taguchi, T. *Tetrahedron* **2005**, *61*, 5741.

10.1021/ol052781k CCC: $33.50
Published on Web 01/24/2006

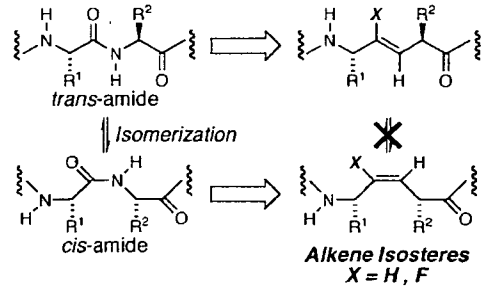

Figure 1. *Cis/trans* equilibrium of peptide bond and the corresponding alkene- or fluoroalkene isosteres.

and resist enzymatic degradation. Peptide bonds exist in *cis/trans* equilibrium, while alkene isosteres serve as defined *trans*-amide or *cis*-amide equivalents, which do not isomerize to each other. *Cis/trans* isomerization of peptide bonds (especially Xaa-Pro sequences) in several bioactive peptides tends to play an important role in their conformations and biological activities.[5] Therefore, alkene and fluoroalkene isosteres might be promising tools for conformational analysis of bioactive peptides and proteins.[6] We have been engaged in the development of synthetic methodologies for (*E*)-alkene or (*Z*)-fluoroalkene dipeptide isosteres as *trans*-amide bond equivalents utilizing organocopper reagents or SmI_2. However, the lack of efficient synthetic methodologies for the preparation of (*Z*)-alkene or (*E*)-fluoroalkene dipeptide isosteres as *cis*-amide bond equivalents has limited an extensive application of alkene and fluoroalkene isosteres in the analysis of amide bond geometries in bioactive peptides and proteins. In this paper, we describe a new synthetic approach for the preparation of (*Z*)-alkene or (*E*)-fluoroalkene dipeptide isosteres. We also include the application of these isosteres to probe structural requirements of the peptide transporter PEPT1.

Our synthetic routes for the preparation of (*Z*)-alkene and (*E*)-fluoroalkene isosteres are depicted in Scheme 1. We envisioned key synthetic intermediates **B** would be synthesized by organocopper-mediated reduction of lactam **A** with predominant formation of β,γ-(*Z*)-alkenes or (*E*)-fluoroalkenes as *cis*-amide equivalents. This strategy could be expanded into consecutive one-pot reduction/α-alkylation methodologies for the synthesis of structurally diverse α-alkylated (*Z*)-alkene and (*E*)-fluoroalkene dipeptide isosteres.[7] First, we synthesized γ-acetoxy- or γ,γ-difluoro-α,β-unsaturated lactams and examined the organocopper-mediated reduction of these substrates to confirm whether this approach was applicable to the synthesis of *cis*-amide bond isosteres.

Guibé et al. reported a similar but inherently different convergent approach to the synthesis of (*Z*)-alkene isosteres

Scheme 1. Synthetic Route for (*Z*)-Alkene and (*E*)-Fluoroalkene Dipeptide Isosteres

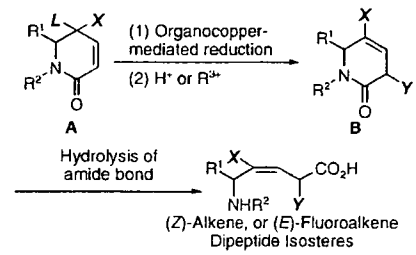

L: leaving group (OAc or F). *X*: H or F. *Y*: H or R^3.

via 3,6-dihydropyridin-2-ones, in which the β,γ-(*Z*)-alkene unit was constructed by Grubbs' RCM after condensation of chiral allylamines with chiral vinyl acetic acids.[8] The present method provides a new entity for the synthesis of (*Z*)-alkene isosteres in a divergent fashion. That is complementary to their method as well as our alternative method based on organocoper-mediated *anti*-S_N2' reaction.[9] It is noteworthy that to our knowledge, this is the first unequivocal synthesis of (*E*)-fluoroalkene dipeptide isosteres.

Substrates for the organocopper-mediated reduction were synthesized by the sequence of reactions shown in Scheme 2. Synthesis of acetate **6** started from a known phenylalanine derivative **1**.[9] Conversion of the *N*-protecting group of **1** to *N*-Ns (Ns = 2-nitrobenzenesulfonyl)[10] followed by *O*-protection with a TBS group gave *N*-Ns amide derivative **2**. Treatment of **2** with DMB (2,4-dimethoxybenzyl) alcohol under Mitsunobu conditions afforded the *N*-DMB sulfonamide **3**. After removal of the *N*-Ns group of **3**, acylation of the resulting secondary amine followed by *O*-TBS deprotection gave the acrylamide derivative **4**. RCM reaction of **4** with Grubbs' ruthenium catalyst[11] proceeded smoothly at room temperature to yield the γ-hydroxy-α,β-unsaturated δ-lactam **5**. Lactam **5** was converted to acetate **6** by Ac_2O treatment in the presence of pyridine.

γ,γ-Difluoro-α,β-unsaturated δ-lactam **12** was synthesized from the β-amino ester **10**, which was prepared from phenylacetaldehyde **7** and the chiral amine **8** via rhodium catalized diastereoselective Reformatsky–Honda reaction.[4d,12] After DIBAL-H treatment of **10**, (*Z*)-selective Horner–Wadsworth–Emmons reaction[13] of the resulting aldehyde gave (*Z*)-enoate **11** in 72% yield with a concomitant formation of small amount of (*E*)-isomer (4%). After deprotection of the Boc and *t*-Bu groups of **11** using 4 M HCl in dioxane, cyclization with EDC gave the desired lactam **12**.

(5) Dugave, C.; Demange, L. *Chem. Rev.* **2003**, *103*, 2475.
(6) Wang, X. J.; Xu, B.; Mullins, A. B.; Neiler, F. K.; Etzkorn, F. A. *J. Am. Chem. Soc.* **2004**, *126*, 15533.
(7) Otaka, A.; Watanabe, H.; Yukimasa, A.; Oishi, S.; Tamamura, H.; Fujii, N. *Tetrahedron Lett.* **2001**, *42*, 5443, and references cited therein.
(8) Boucard, V.; S.-Dorizon, H.; Guibé, F. *Tetrahedron* **2002**, *58*, 7275.
(9) Niida, A.; Oishi, S.; Sasaki, Y.; Mizumoto, M.; Tamamura, H.; Fujii, N.; Otaka, A. *Tetrahedron Lett.* **2005**, *46*, 4183.
(10) Fukuyama, T.; Jow, C.-K.; Cheung, M. *Tetrahedron Lett.* **1995**, *36*, 6373.
(11) Scholl, M.; Ding, S.; Lee, C. W.; Grubbs, R. H. *Org. Lett.* **1999**, *1*, 953.
(12) Honda, T.; Wakabayashi, H.; Kanai, K. *Chem. Pharm. Bull.* **2002**, *50*, 307.
(13) Ando, K.; Oishi, T.; Hirama, M.; Ohno, H.; Ibuka, T. *J. Org. Chem.* **2000**, *65*, 4745.

Scheme 2. Synthesis of Requisite Substrates for Organocopper-Mediated Reduction

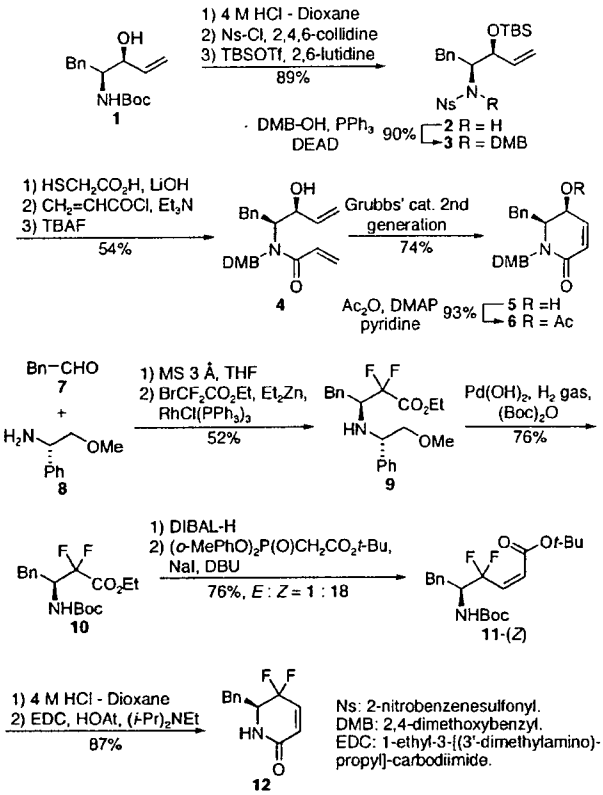

Next we examined the organocopper-mediated reduction of lactams **6** and **12** (Scheme 3). The reaction of acetate **6** with Me_3CuLi_2·LiI·3LiBr[14] proceeded smoothly at −78 °C to yield the β,γ-unsaturated lactam **13** in a good yield (88%). The DMB group of lactam **13** was easily removed using TFA. Treatment of difluorolactam **12** with Me_3CuLi_2·LiI·3LiBr also gave the desired reduction product **15** in excellent yield (92%).

Scheme 3. Synthesis of Phe-Gly Type (*Z*)-Alkene- and (*E*)-Fluoroalkene Dipeptide Isosteres via Organocopper-Mediated Reduction of Lactams **6** and **12**

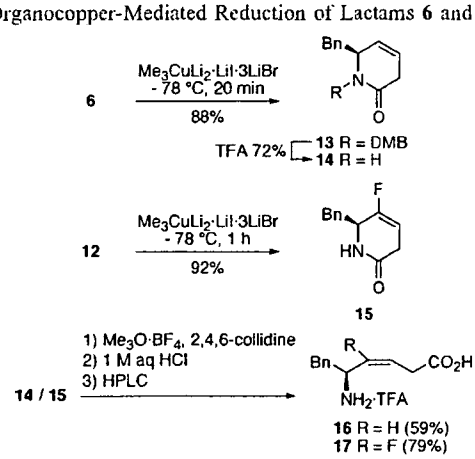

Next, we carried out the hydrolysis of the amide bond in lactams **14** and **15** to accomplish the synthesis of the *cis*-amide bond isosteres. Lactams **14** and **15** were converted to lactim ethers using $Me_3O·BF_4$. Hydrolysis of the lactim ethers[15] under acidic conditions followed by HPLC purification using 0.1% TFA aqueous MeCN gave Phe-Gly type (*Z*)-alkene dipeptide isostere (Phe-ψ[(*Z*)-CH=CH]-Gly **16**) and (*E*)-fluoroalkene dipeptide isostere (Phe-ψ[(*E*)-CF=CH]-Gly **17**),[16] respectively as TFA salts.

The above organocopper-mediated reduction is applicable to consecutive one-pot α-alkylation (Scheme 4). After reduction of lactam **6** with Me_3CuLi_2·LiI·3LiBr, the resulting metal enolate was trapped by Bn-Br to yield the *trans*-α-substituted diketopiperazine mimetic **18** as a main product. After deprotection of the DMB group using TFA, the resulting lactam **19** was subjected to ring-opening followed by *N*-Boc protection to yield Boc-L-Phe-ψ[(*Z*)-CH=CH]-D-Phe-OMe **20** in 40% yield with a small amount of α-epimerized product (13%). Boc-D-Phe-ψ[(*E*)-CF=CH]-L-Phe-OMe **23** was also synthesized from lactam **21** by a procedure

Scheme 4. Synthesis of α-Substituted (*Z*)-Alkene and (*E*)-Fluoroalkene Dipeptide Isosteres Utilizing Organocopper-Mediated Reduction−Alkylation

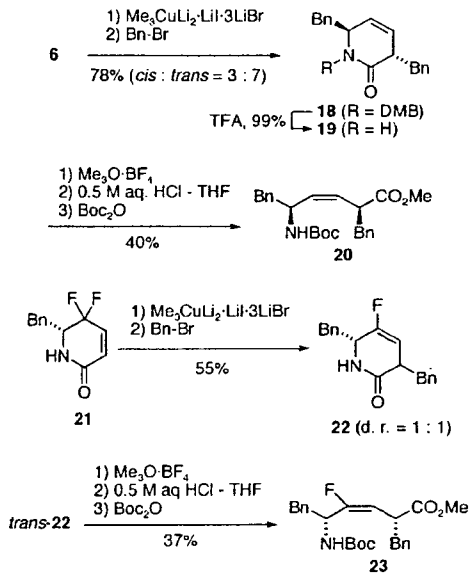

(14) Single electron transfer (SET) mechanism has been proposed as one of the plausible mechanisms of organocopper-mediated reduction. The electron-transfer potency of Me_3CuLi_2 was proved to be higher than that of the corresponding Gilman-type reagent such as Me_2CuLi. See: Chounan, Y.; Horino, H.; Ibuka, T.; Yamamoto, Y. *Bull. Chem. Soc. Jpn.* **1997**, *70*, 1953.

(15) Schöllkopf, U.; Hartwig, W.; Pospischil, K.-H.; Kehne, H. *Synthesis* **1981**, 966.

(16) Coupling constants of **17** and **23** ($^3J_{HF}$ = 20.7 and 20.5 Hz, respectively) are consistent with those of α-fluorovinyl groups possessing a (*E*)-configuration ($^3J_{HF\,trans}$ = 18−22 Hz). See ref 4b.

similar to that for the synthesis of isostere **20**.[17] Precise stereocontrol and introduction of other functional groups at the α-position are under investigation.

Next, we investigated whether the di/tri-peptide transporter, PEPT1 recognized synthetic Phe-Gly type isosteres as substrates. PEPT1 is a membrane protein which has 12 transmembrane domains and mediates intestinal uptake of not only di-/tripeptides but also several drugs structually related to small peptides such as β-lactam antibiotics.[18] Structure–activity relationship studies of various substrates for PEPT1 have been carried out in order to apply this transporter to develop orally bio-available drugs. However precise recognition mechanisms have not been elucidated. We envisioned that alkene dipeptide isosteres would be useful tools for analysis of recognition mechanisms of PEPT1 because of their structural similarity to parent dipeptides. We also expected that the potency of dipeptide isosteres as amide bond mimetics could be evaluated by use of the PEPT1 dipeptide transport system.

The bioactivities of synthetic Phe-Gly isosteres for PEPT1 were determined by the inhibition of [^{3}H]Gly-Sar uptake in PEPT1-expressing Caco-2 cell in comparison with *trans*-amide type isosteres, **24**, **25**, and other related compounds (see the Supporting Information attached). Inhibition constants (K_i) of parent dipeptide Phe-Gly and its isosteres are shown in Table 1. *trans*-Amide equivalents **24** and **25** possessed good affinity for PEPT1 corresponding to the parent dipeptide (K_i: Phe-Gly, 0.205 mM; **24**, 0.853 mM; **25**, 1.34 mM). It is of note that affinities of the *cis*-amide equivalents **16** and **17** for PEPT1 were more than 10 times weaker than those of *trans*-isomers. These data suggest that PEPT1 predominantly recognizes *trans*-amide conformations of dipeptides. This is in good accordance with the previous report by Brandsch et al., in which PEPT1 recognized *trans*-conformation of Ala-ψ[CS–N]-Pro.[19] Conformationally flexible analogues **26** and **27** retained moderate affinity in comparison with *cis*-amide equivalents. Presumably, analogues **26** and **27** could exist as *trans*-amide-like conformers, which were favorable for the interaction with PEPT1, due to their flexibility. Contrary to our expectation, an increase of affinity by the introduction of fluoroalkene unit was not observed (**24** vs **25**). Further investigation is required for verification of the effect of fluorine as a carbonyl oxygen mimic.

Table 1. K_i Values of Phe-Gly and Various Isosteres Based on Inhibition of [^{3}H]Gly-Sar Uptake by PEPT1 in Caco-2 Cell

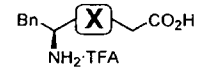

compd	X	K_i (mM)
Phe-Gly	–CO-NH–	0.205
16	–ψ[(*Z*)-CH=CH]–	>10.0
17	–ψ[(*E*)-CF=CH]–	>10.0
24	–ψ[(*E*)-CH=CH]–	0.853
25	–ψ[(*Z*)-CF=CH]–	1.34
26	–ψ[CH_2-CH_2]–	2.17
27	–ψ[CF_2-CH_2]–	1.67

In conclusion, we presented a novel unambiguous synthetic route for the syntheses of (*Z*)-alkene and (*E*)-fluoroalkene dipeptide isosteres as *cis*-amide bond mimetics via organocopper-mediated reduction of γ-acetoxy- or γ,γ-difluoro-α,β-unsaturated δ-lactams. We also carried out comparative studies of affinities for peptide transpoter PEPT1 between the *cis*-amide mimetics and the corresponding *trans*-amide isosteres, and found that peptide transporter PEPT1 predominantly recognizes *trans*-amide bond conformations in dipeptides. Synthetic studies on various α-substituted (*E*)-fluoroalkene isosteres and further structure–activity-relationship studies on dipeptide mimetics for PEPT1 are currently proceeding.

Acknowledgment. We thank Dr. Terrence R. Burke, Jr., NCI, NIH, for proofreading this manuscript. This research was supported in part by 21st Century COE Program "Knowledge Information Infrastructure for Genome Science", a Grant-in-Aid for Scientific Research from the Ministry of Education, Culture, Sports, Science and Technology, Japan, the Japan Society for the Promotion of Science (JSPS), and the Japan Health Science Foundation. A.N. is grateful for Research Fellowships from the JSPS for Young Scientists.

Supporting Information Available: Synthesis of compounds **24**–**27**. Experimental procedures and spectral data. This material is available free of charge via the Internet at http://pubs.acs.org.

OL052781K

(17) In ^{1}H NMR experiments, α-protons (position-3) of 3,6-*trans* isomers such as **18** or *trans*-**22** appeared upfield from the corresponding α-protons of 3,6-*cis* isomeres. See ref 9.

(18) (a) Våbenø, J.; Lejon, T.; Nielsen, C. U.; Steffansen, B.; Chen, W.; Ouyang, H.; Borchardt, R. T.; Luthman, K. *J. Med. Chem.* **2004**, *47*, 1060. (b) Våbenø, J.; Nielsen, C. U.; Ingebrigtsen, T.; Lejon, T.; Steffansen, B.; Luthman, K. *J. Med. Chem.* **2004**, *47*, 4755. (c) Terada, T.; Inui, K. *Curr. Drug Metab.* **2004**, *5*, 85. (d) Biegel, A.; Gebauer, S.; Hartrodt, B.; Brandsh, M.; Neubert, K.; Thondorf, I. *J. Med. Chem.* **2005**, *48*, 4410.

(19) Brandsh, M.; Thunecke, F.; Küllertz, G.; Schutkowski, M.; Fischer, G.; Neubert, K. *J. Biol. Chem.* **1998**, *273*, 3861.

ORGANIC LETTERS
2006
Vol. 8, No. 3
467–470

Cysteine-Derived *S*-Protected Oxazolidinones: Potential Chemical Devices for the Preparation of Peptide Thioesters

Yusuke Ohta,[†] Saori Itoh,[†] Akira Shigenaga,[‡] Saori Shintaku,[‡] Nobutaka Fujii,[†] and Akira Otaka*[,†,‡]

Graduate School of Pharmaceutical Sciences, Kyoto University, Sakyo-ku, Kyoto 606-8501, Japan, and Graduate School of Pharmaceutical Sciences, The University of Tokushima, Shomachi, Tokushima 770-8505, Japan

aotaka@ph.tokushima-u.ac.jp

Received November 14, 2005

ABSTRACT

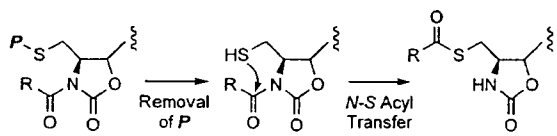

An *N–S* acyl-transfer-mediated preparation of peptide thioesters using the *S*-protected oxazolidinone derived from cysteine has been developed and applied to the synthesis of a 32-mer biologically active peptide by native chemical ligation protocols.

Intein-mediated protein splicing is a self-catalytic editing system of proteins in which an intervening sequence (termed "intein") is cleaved off from a protein precursor with simultaneous ligation between the flanking fragments (*N*- and *C*-exteins) to form a mature extein protein and the free intein.[1] These intein-mediated splicing systems have received increasing attention in the field of protein chemistry including purification,[2] labeling,[3] and semisynthesis of proteins.[4] In this splicing process, three consecutive acyl-transfer steps are involved.[5] The first *N*−*S* acyl transfer on the cysteine residue at intein *N*-terminus has been extensively applied to the biochemical preparation of protein (or peptide) thioesters. These have shown great utility in the preparation of a wide variety of proteins by native chemical ligation (NCL) procedures.[4,6] Therefore, we anticipated that mimicking the intein-mediated *N*−*S* acyl-transfer step by chemical means could provide an unprecedented alternative to reported chemical methods for the synthesis of peptide thioesters.[7] A recent elegant NMR study[8] on this acyl transfer revealed that "ground-state destabilization" by inducing nonplanarity in the scissile amide bond was responsible for activation of the

[†] Kyoto University.
[‡] The University of Tokushima.

(1) For protein splicing bibliography, see: (a) Perler, F. B. *Nucleic Acids Res.* **2002**, *30*, 383−384. (b) http://www.neb.com/neb/inteins.html.

(2) (a) Chong, S.; Mersha, F. B.; Comb, D. G.; Scott, M. E.; Landry, D.; Vence, L. M.; Perler, F. B.; Benner, J.; Kucera, R. B.; Hirvonen, C. A.; Pelletier, J. J.; Paulus, H.; Xu, M. *Gene* **1997**, *192*, 271−281. (b) Chong, S.; Montello, G. E.; Zhang, A.; Cantor, E. J.; Liao, W.; Xu, M. Q.; Benner, J. *Nucleic Acids Res.* **1998**, *26*, 5109−5115. (c) Evans, T. C., Jr.; Benner, J.; Xu, M. Q. *J. Biol. Chem.* **1999**, *274*, 3923−3926.

(3) (a) Miller, L. W.; Cornish, V. W. *Curr. Opin. Chem. Biol.* **2005**, *9*, 56−61. (b) Zuger, S.; Iwai, H. *Nat. Biotechnol.* **2005**, *23*, 736−740. (c) Girish, A.; Sun, H.; Yeo, D. S.; Chen, G. Y.; Chua, T. K.; Yao, S. Q. *Bioorg. Med. Chem. Lett.* **2005**, *15*, 2447−2451.

(4) (a) Alexandrov, K.; Heinemann, I.; Durek, T.; Sidorovitch, V.; Goody, R. S.; Waldmann, H. *J. Am. Chem. Soc.* **2002**, *124*, 5648−5649. (b) Muir, T. W. *Annu. Rev. Biochem.* **2003**, *72*, 249−289. (c) Clayton, D.; Shapovalov, G.; Maurer, J. A.; Dougherty, D. A.; Lester, H. A.; Kochendoerfer, G. G. *Proc. Natl. Acad. Sci. U.S.A.* **2004**, *101*, 4764−4769. (d) Machova Z.; Beck-Sickinger, A. G. *Methods Mol. Biol.* **2005**, *298*, 105−135.

(5) (a) Poland, B. W.; Xu, M. Q.; Quiocho, F. A. *J. Biol. Chem.* **2000**, *275*, 16408−16413. (b) Evans, T. C.; Xu, M. Q. *Chem. Rev.* **2002**, *102*, 4869−4884.

(6) (a) Dawson, P. E.; Muir, T. W.; Clark-Lewis, I.; Kent, S. B. H. *Science* **1994**, *266*, 776−779. (b) Dawson, P. E.; Kent, S. B. H. *Annu. Rev. Biochem.* **2000**, *69*, 923−960.

10.1021/ol052755m CCC: $33.50
Published on Web 01/10/2006

amide leading to the $N-S$ acyl transfer.[9] On the basis of this finding, we attempted to use an N-acyloxazolidinone derivative to prepare thioesters by a "ground-state destabilization" mechanism. In an acyloxazolidinone, the carbonyl in the oxazolidinone ring is likely to influence the $n_N-\pi^*_{CO}$ delocalization and to result in the activation (ground-state destabilization) of the *exo*-amide linkage. Actually, N-acyloxazolidinones have been documented to show active ester character which is regulated by distortion of the amide planarity.[10] Because neighboring thiol group participation in the cleavage of the acyloxazolidinone bond could facilitate the formation of thioesters,[11] an S-protected oxazolidinone derived from cysteine was selected as a chemical device for the preparation of peptide thioesters by an intein mimicking mechanism. In this study, we examined the applicability of cysteine-derived acyloxazolidinones to the $N-S$ acyl shift-mediated synthesis of peptide thioesters with application to peptide synthesis using NCL.[12] Very recently, two groups have reported $N-S$ acyl-transfer-mediated preparation of peptide thioesters using chemical devices other than the oxazolidinones.[13,14]

The use of S-protected oxazolidinones in the synthesis of peptide thioesters is conceptually outlined in Figure 1. A

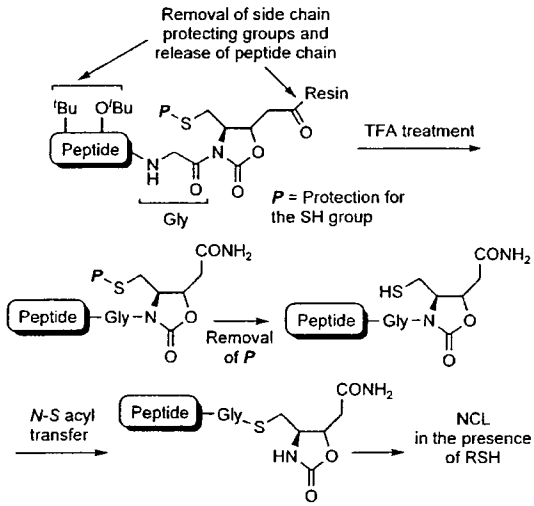

Figure 1. Concept of $N-S$ acyl transfer-mediated synthesis of peptide thioesters using an S-protected oxazolidinone.

protected peptide chain is assembled on the S-protected oxazolidinone-type linker by solid-phase peptide synthesis (SPPS) followed by removal of protecting groups except for the S-protection on the oxazolidinone. Concomitant release of the peptidyloxazolidinone from the resin yields the S-protected peptide oxazolidinone as a precursor to the thioester. Removal of the S-protection and subsequent $N-S$ acyl transfer affords the peptide thioester.

The p-methoxybenzyl (MBzl) group was selected as an oxazolidinone S-protecting group because it remains intact during standard Fmoc-based SPPS protocols (20% piperidine treatment for Fmoc-removal and trifluoroacetic acid (TFA) treatment for the final deprotection). Preparation of a protected oxazolidinone derivative suitable for attaching to an amino-functionalized resin and its use in the synthesis of the peptide thioester precursor are shown in Scheme 1.

Scheme 1

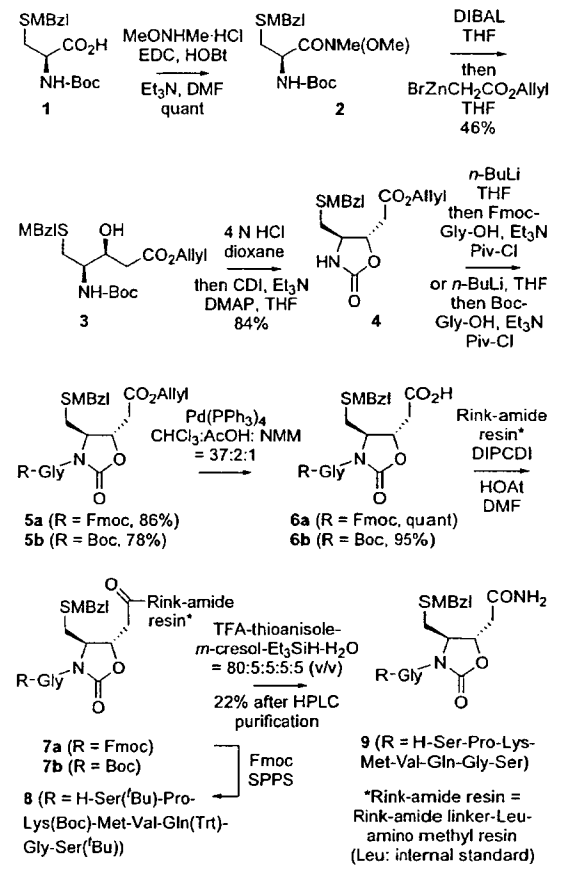

Starting from the protected cysteine derivative **1**, *syn*-1,2-amino alcohol derivative **3** was obtained exclusively by a sequence of reactions consisting of Weinreb-amidation using 1-ethyl-3-(3-dimethylaminopropyl)carbodiimide (EDC),[15] diisobutylaluminum hydride (DIBAL) reduction, and Refor-

(7) For synthesis of peptide thioesters using Boc strategy, see: (a) Aimoto, S. *Biopolymers* **1999**, *51*, 247–265. (b) Hackeng, T. M.; Griffin, J. H.; Dawson, P. E. *Proc. Natl. Acad. Sci. U.S.A.* **1999**, *96*, 10068–10073. For synthesis of peptide thioesters using the Fmoc strategy, see: (c) Ingenito, R.; Bianchi, E.; Fattori, D.; Pessi, A. *J. Am. Chem. Soc.* **1999**, *121*, 11369–11374. (d) Shin, Y.; Winans, K. A.; Backes, B. J.; Kent, S. B. H.; Ellman, J. A.; Bertozzi, C. R. *J. Am. Chem. Soc.* **1999**, *121*, 11684–11689. (e) Sewing, A.; Hilvert, D. *Angew. Chem., Int. Ed.* **2001**, *40*, 3395–3396. (f) Brask, J.; Albericio, F.; Jensen, K. J. *Org. Lett.* **2003**, *5*, 2951–2953.

(8) Romanelli, A.; Shekhtman, A.; Cowburn, D.; Muir, T. W. *Proc. Natl. Acad. Sci. U.S.A.* **2004**, *101*, 6397–6402.

(9) Mujika, J. I.; Mercero, J. M.; Lopez, X. *J. Am. Chem. Soc.* **2005**, *127*, 4445–4453.

(10) Evans, D. A.; Anderson, J. C.; Taylor, M. K. *Tetrahedron Lett.* **1993**, *34*, 5563–5566.

matsky reaction of allyl bromoacetate. Deprotection of the Boc group of **3** with 4 N HCl–dioxane followed by carbonyldiimidazole (CDI)/4-(dimethylamino)pyridine (DMAP)-mediated cyclization of the resulting deprotected compound afforded the *S*-MBzl oxazolidinone **4**. Acylation of lithiated **4** with Fmoc-Gly-OH in the presence of pivaloyl chloride (Piv-Cl) and Et_3N gave the Fmoc-glycyloxazolidinone **5a**. For attachment of the acyloxazolidinone to the resin, allyl ester on **5a** was quantitatively removed by treatment with $Pd(PPh_3)_4$ in $CHCl_3$/AcOH/*N*-methylmorpholine (NMM) (37:2:1, v/v).[16]

The resulting carboxylic acid **6a** can be coupled to an amino-functionalized resin using standard peptide coupling conditions. Before elongation of the peptide chain, the stability of the acyloxazolidinone linkage toward basic treatment needed for Fmoc-removal was examined. For this purpose, Rink amide linker-functionalized resin possessing an internal standard amino acid (Leu) for amino acid analysis following acid hydrolysis was prepared by successive coupling of Fmoc-Leu-OH and Fmoc-Rink linker[17] on the amino methyl resin. On this resin was coupled the Boc-glycyloxazolidinone **6b**, which was prepared by reactions identical to those used for **6a**. Treatment of the resulting resin **7b** with basic reagent systems followed by amino acid analysis after acid hydrolysis indicated that treatment with 20% piperidine in *N,N*-dimethylformamide (DMF) (standard Fmoc deprotection) partially induced the decomposition of the amide linkage (ca. 20% of the linkage was broken after 5 h treatment). On the other hand, the use of Aimoto's reagent mixture[18] consisting of 1-methylpyrrolidine-hexamethyleneimine-1-hydroxybenzotriazole (HOBt) (25% (v/v)–2% (v/v)–3% (w/v) in 1-methylpyrrolidin-2-one (NMP)-dimethyl sulfoxide (DMSO) (1:1)) proved to be compatible with the resin in the presence of the acyloxazolidinone linkage.[19] This basic reagent system has been successfully applied to the Fmoc-based synthesis of peptide thioesters without affecting thioester linkages. However, one potential limitation with the use of this procedure in the synthesis of thioesters is racemization of chiral thioester-linked *C*-terminal amino acids.[20] This is the case with aminoacylated oxazolidinones.[21] At this stage, since only Fmoc-glycyloxazolidinone such as **6a** can be applicable to the *N–S* acyl-transfer-mediated methodology, extensive efforts are in progress in our laboratory to develop deprotection conditions suitable for chiral *C*-terminal aminoacylated oxazolidinones.

Next, to evaluate the practical usefulness of **6a** in application to the NCL-mediated preparation of peptides, we undertook the synthesis of hBNP32-NH_2 **14**. The peptide chain assembly for the peptide thioester precursor fragment **9** (corresponding to hBNP32-NH_2 (1–9)) was conducted using the Fmoc-Rink linker-Leu resin, on which Fmoc-glycyloxazolidinone **6a** and Fmoc-amino acids were successively coupled with the aid of diisopropylcarbodiimide (DIPCDI)-HOBt (or 1-hydroxy-7-azabenzotriazole (HOAt)). Treatment with Aimoto's reagent cocktail (20 min reaction/each step) was utilized for the removal of Fmoc groups. Amino acid analysis of the hydrolysate resulting from the completed resin **8** revealed that the peptide chain assembly proceeded efficiently without significant decomposition of the acyloxazolidinone linkage.[22] Treatment of the completed resin **8** with TFA–thioanisole–*m*-cresol–Et_3SiH–H_2O (80:5:5:5:5, v/v) at room temperature for 2 h, followed by HPLC purification, gave the *S*-protected peptidyloxazolidinone **9** as a thioester precursor in 22% yield.

The resulting peptidyloxazolidinone was then subjected to the NCL-mediated synthesis of hBNP32-NH_2 (Scheme 2). HPLC-purified *S*-protected derivative **9** was treated with

Scheme 2

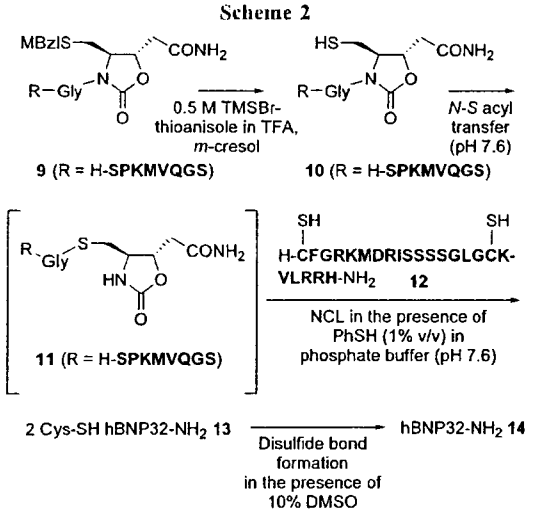

0.5 M trimethylsilyl bromide (TMSBr)–thioanisole (1:1) in TFA and *m*-cresol[23] at −10 °C for 1 h to afford the *S*-deprotected peptidyloxazolidinone **10**, which was then purified by HPLC. NCL of the purified **10** with the

(11) For nucleophilic involvement of hydroxy group leading to *N–O* acyl transfer, see: Bew, S. P.; Bull, S. D.; Davies, S. G.; Savory, E. D.; Watkin, D. J. *Tetrahedron* **2002**, *58*, 9387–9401 and references cited herein.

(12) A 32-mer disulfide-containing peptide, human brain natriuretic peptide derivative (amide form: hBNP32-NH_2 **14**), was selected as model synthetic peptide. For hBNP32, see: Kambayashi, Y.; Nakao, K.; Mukoyama, M.; Saito, Y.; Ogawa, Y.; Shiono, S.; Inoue, K.; Yoshida, M.; Imura, H. *FEBS Lett.* **1990**, *259*, 341–345.

(13) Olliver, N.; Behr, H.-B.; El-Mahdi, O.; Blanpain, A.; Melnyk, O. *Org. Lett.* **2005**, *7*, 2647–2650.

(14) Kawakami, T.; Sumida, M.; Nakamura, K.; Vorherr, T.; Aimoto, S. *Tetrahedron Lett.* **2005**, *46*, 8805–8807.

(15) Wang, G.; Mahesh, U.; Chen, G. Y. J.; Yao, S. Q. *Org. Lett.* **2003**, *5*, 737–740 and references cited herein.

(16) Kates, S. A.; Daniels, S. B.; Sole, N. A.; Barany, G.; Albericio, F. In *Peptides: Chemistry, Structure and Biology*; Hodges, R. S., Smith, J. A., Eds.; ESCOM: Leiden, 1994; pp 113–115.

(17) Bernatowicz, M. S.; Daniels, S. D.; Kster, H. *Tetrahedron Lett.* **1989**, *30*, 4645–4648.

(18) Li, X. Q.; Kawakami, T.; Aimoto, S. *Tetrahedron Lett.* **1998**, *39*, 8669–8672.

(19) Treatment of **7b** with Aimoto's reagent cocktail for 5 h induced ca. 3% cleavage of the linkage. See the Supporting Information.

(20) Hasegawa, K.; Sha, Y. L.; Bang, J. K.; Kawakami, T.; Akaji, K.; Aimoto, S. *Lett. Peptide Sci.* **2002**, *8*, 277–284.

(21) Oxazolidinone derivative **4** was derivatized with Fmoc-L-Ala-OH. Then, treatment of the resulting Fmoc-L-Ala-linked derivative with the Aimoto's reagent cocktail afforded the mixture of H-L-Ala- or H-D-Ala-linked oxazolidinone derivative. Results of quantitative HPLC analysis of the reaction mixture are shown as a graph in the Supporting Information.

N-terminal cysteine peptide (hBNP32-NH_2 (10−32)) **12**, which was prepared by standard Fmoc-based peptide synthesis, proceeded efficiently in phosphate buffer (pH 7.6) containing 6 M guanidine·HCl in the presence of 1% (v/v) thiophenol to yield the ligated 2Cys-SH hBNP32-NH_2 **13**. At this step in the NCL protocol, the *N*-acylated compound **10** (retention time on HPLC analysis = 10.8 min) disappeared completely within 1 min and a new compound (putatively **11**) with the same *m/z* value as that of **10** eluted at 7.8 min (see the Supporting Information).[24] After dilution with phosphate buffer to three times volume, DMSO (10%, v/v) was added to effect disulfide bond formation.[25] HPLC purification of the crude product gave purified hBNP32-NH_2 **14** in 78% yield calculated from the NCL step.

Based on the reaction mechanism of intein-mediated formation of peptide thioesters, we have developed a method for *N*−*S* acyl-transfer-mediated synthesis of thioesters using acylated oxazolidinones derived from *S*-protected cysteine. Removal of peptidyloxazolidinone *S*-protection provides the corresponding peptide thioesters through *N*−*S* acyl transfer involving the thiol group in the adjacent activated acyl-oxazolidinone linkage. This synthetic protocol was successfully applied to the NCL-mediated synthesis of hBNP32-NH_2. The use of cysteine-derived oxazolidinones as chiral auxiliaries with application to the preparation of thioesters could provide a new access to chiral thioester derivatives, which could have potential utility in the synthesis of a wide variety of compounds.

Acknowledgment. We thank Dr. Terrence R. Burke, Jr., NCI, NIH, for proofreading this manuscript. This research was supported in part by the 21st Century COE Program "Knowledge Information Infrastructure for Genome Science", a Grand-in-Aid for Scientific Research (KAKENHI). A.O. is grateful for research grants from Sekisui Integrated Research and Suzuken Memorial Foundation.

Supporting Information Available: Experimental procedures, NMR charts for key compounds, and HPLC charts of the analyses of *N*−*S* acyl-transfer-mediated synthesis of hBNP32-NH_2. This material is available free of charge via the Internet at http://pubs.acs.org.

OL052755M

(22) The decomposition of the acyloxazolidinone linkage is attributed to both base-induced cleavage of the activated bond (ca. 3% decomposition after 5 h treatment)[19] and diketopiperazine (DKP) formation. These two factors were probably responsible for the partial loss of peptide chain (Glu (in the peptide)/Leu (in the solid support) = 0.9:1.0). We have yet to prove to attribute the loss to the base-induced cleavage, DKP formation, or precision in amino acid analysis.

(23) Yajima, H.; Fujii, N.; Funakoshi, S.; Watanabe, T.; Murayama, E.; Otaka, A. *Tetrahedron* **1988**, *44*, 805−819.

(24) Removal of the thiol protection is needed for the coupling with *N*-terminal cysteine peptide. Subjection of *S*-protected peptidyloxazolidinone such as **9** to the NCL condition does not afford the ligated product.

(25) (a) Otaka, A.; Koide, T.; Shide, A.; Fujii, N.; *Tetrahedron Lett*, **1990**, *32*, 1223−1226; Tam, J. P.; Wu, C.; Liu, W.; Zhang, J. *J. Am. Chem. Soc.* **1991**, *113*, 6657−6662. (c) Ueda, S.; Fujita, M.; Tamamura H.; Fujii, N.; Otaka, A. *ChemBioChem* **2005**, *6*, 1983−1986.

Involvement of the CXCL12/CXCR4 Pathway in the Recovery of Skin Following Burns

Shani Avniel[1,9], Zaretski Arik[2,9], Alex Maly[3], Assa Sagie[2], Hanna Ben Basst[4], Merav Darash Yahana[1], Ido D. Weiss[1], Boaz Pal[1], Ori Wald[1], Dean Ad-El[5], Nobutaka Fujii[6], Fernando Arenzana-Seisdedos[7], Steffen Jung[8], Eithan Galun[1], Eyal Gur[2] and Amnon Peled[1]

Burn wound healing is a complex process consisting of an inflammatory phase, the formation of granulation tissue, and remodeling. The role of the CXCL12/CXCR4 pathway in the recovery of skin following burns is unknown. We found that CXCL12 is similarly expressed in human, swine, and rat skin by pericyte and endothelial cells, fibrous sheet, fibroblasts, and axons. Following burns, the levels of CXCL12 were markedly increased in human burn blister fluids. One day after injury, there was a gradual increase in the expression of CXCL12 in the hair follicles and in blood vessel endothelium surrounding the burn. Three to 11 days following burns, an increased number of fibroblasts expressing CXCL12 were observed in the recovering dermis of rat, swine, and human skin. In contrast to CXCL12, CXCR4 expression was detected in proliferating epithelial cells as well as in eosinophils and mononuclear cells infiltrating the skin. *In vitro*, CXCL12 was expressed by primary human skin fibroblasts, but not by keratinocytes, and was stimulated by wounding a confluent cell layer of these fibroblasts. Blocking the CXCR4/CXCL12 axis resulted in the significant reduction in eosinophil accumulation in the dermis and improved epithelialization. Thus, blocking CXCR4/CXCL12 interaction may significantly improve skin recovery after burns.

Journal of Investigative Dermatology (2006) **126**, 468–476. doi:10.1038/sj.jid.5700069; published online 22 December 2005

INTRODUCTION

Skin integrity is of importance for the protection and separation of body tissues from the surrounding environment. The loss of skin due to burns or trauma exposes the body to severe stress, impairing or even eliminating the many vital functions this organ performs (Clark, 1988; Cotran *et al.*, 1999). Full-thickness skin tissue is comprised of keratinocytes lined on a basement membrane, produced by fibroblasts and keratinocytes. Deeper layers of the skin include, in addition to fibroblasts, fat cells and multiple subsets of immune cells such as dendritic cells, lymphocytes, and polymorphonuclear cells. The complex organization of normal skin is designed to support the numerous functions of this organ as both an immunologic and a physical barrier. Nevertheless, not much is known about the factors responsible for the complex architecture of this organ under physiologic and pathologic conditions.

Stromal-derived factor-1 (CXCL12) controls many aspects of stem cell function. CXCL12 has been identified as a powerful chemoattractant for immature hematopoietic stem cells (Aiuti *et al.*, 1997). Mice that lack either CXCL12 or its receptor CXCR4 exhibit many defects, including impaired hematopoiesis in the fetal bone marrow (Nagasawa *et al.*, 1996; Ma *et al.*, 1998; Zou *et al.*, 1998; McGrath *et al.*, 1999). Recently, it was shown that mobilization, homing, and engraftment of hematopoietic stem cells as well as the trafficking of neuronal and primordial germ cells are dependent on the expression of CXCL12 and CXCR4 (Peled *et al.*, 1999; Doitsidou *et al.*, 2002). Furthermore, it was also shown that the expression of CXCL12 is upregulated following irradiation and hypoxia and that CXCL12 can induce the recruitment of endothelial progenitor cells in a regeneration model for myocardial infarction (Ponomaryov *et al.*, 2000; Askari *et al.*, 2003; Ceradini *et al.*, 2004). The regulation of CXCL12 and its physiological role in peripheral tissue repair remain incompletely understood. A recent study showed that CXCL12 gene expression is regulated by the transcription factor hypoxia-inducible factor-1 in endothelial cells, resulting in the selective *in vivo* expression of CXCL12 in ischemic tissue in direct proportion to reduced oxygen tension (Hitchon *et al.*, 2002; Schioppa *et al.*, 2003).

[1]*Goldyne Savad Institute of Gene Therapy, Hadassah University Hospital, Jerusalem, Israel;* [2]*Department of Plastic and Reconstructive Surgery, The Tel-Aviv Sourasky Medical Center, Pethach Tikva, Israel;* [3]*Department of Pathology, Hadassah University Hospital, Jerusalem, Israel;* [4]*Laboratory of Experimental Surgery, Hadassah University Hospital, Jerusalem, Israel;* [5]*Department of Plastic and Reconstructive Surgery, Rabbin Medical Center, Pethach Tikva, Israel;* [6]*Graduate School of Pharmaceutical Sciences, Kyoto University, Sakyo-ku, Kyoto, Japan;* [7]*Institute Pasteur, Paris, France and* [8]*Department of Immunology, Weizmann Institute of Science, Rehovot, Israel*

[9]*These authors contributed equally to this work.*

Correspondence: Dr Amnon Peled, Gene Therapy Institute, Hadassah University Hospital, PO Box 12000, Jerusalem, Israel. E-mail: peled@hadassah.org.il or Dr Eyal Gur, Department of Plastic and Reconstructive Surgery, Sourasky Medical Center, PO Box 64239, Tel-Aviv, Israel. E-mail: eyalgur@netvision.net.il

Abbreviations: mAB, monoclonal antibody; GFP, green fluorescent protein

Received 24 March 2005; revised 31 August 2005; accepted 7 September 2005; published online 22 December 2005

Hypoxia-inducible factor-1-induced CXCL12 expression was suggested to increase the adhesion, migration, and homing of circulating CXCR4-positive progenitor cells to ischemic tissue.

Thus, CXCL12 plays an important role in the organization of tissues during development and following damage. CXCL12 is expressed by dendritic cells, fibroblasts, and endothelial cells in human skin (Pablos *et al.*, 1999). Here, we show that following burns, the levels of CXCL12 is markedly increased first in the burn blister and then in the junction tissues surrounding the burn, hair follicles, endothelium blood vessels and fibroblasts in the recovering dermis. Treatment of partial thickness burns in a rat model with antibodies to CXCR4 or the small peptide CXCR4 antagonist, 4F-benzoyl-TN14003 (Tamamura *et al.*, 2003), resulted in improved epithelialization and reduced eosinophilia. These observations suggest a role for eosinophils and the CXCL12/CXCR4 pathway in wound healing and in the recovery of burn skin.

RESULTS

CXCL12 is similarly expressed in human, swine, and rat normal skin

The expression of CXCL12 in normal skin was examined by immunohistochemical staining using monoclonal antibody (mAB) (MAB 350) (R&D Systems Inc., Minneapolis, Minnesota) against the chemokine CXCL12. We first examined the antibody crossreactivity of CXCL12 staining on liver sections of mouse, human, and rat, since previous studies have shown that CXCL12 is specifically expressed in the bile ducts and blood vessels of human liver (Wald *et al.*, 2004). In mouse, human, and rat, liver bile ducts were specifically stained with MAB 350 for CXCL12 (data not shown). Control stain without the primary Ab showed no staining. Using the same mAB staining for CXCL12 in human, swine, and rat, normal skin showed similar expression patterns. CXCL12 in human normal skin (Figure 1) was detected in the basal layer of the epidermis (Figure 1a), on scattered cells in the papillary dermis (Figure 1b), in pericytes, and in the endothelial layer of blood vessels (Figure 1c). The fibrous sheet of hair follicles (Figure 1d), sweat glands (not uniformly) (Figure 1e), axons, and small blood vessels in the nerve tissue (Figure 1f) also expressed CXCL12. No staining was detected with a control antibody used to stain identical skin sections (Figure 1g–h). CXCL12 was detected in rat normal skin on the basal layer of the epidermis (Figure 2a), on scattered cells in the papillary dermis (Figure 2b), and on pericytes and the endothelial layer of blood vessels (Figure 2c). The chemokine CXCL12 was also expressed by axons and small blood vessels in the nerve tissue (Figure 2d) and by fibrous sheet of hair follicles (Figure 2e). No staining was detected with control antibody used to stain the same skin sections (Figure 2f). The

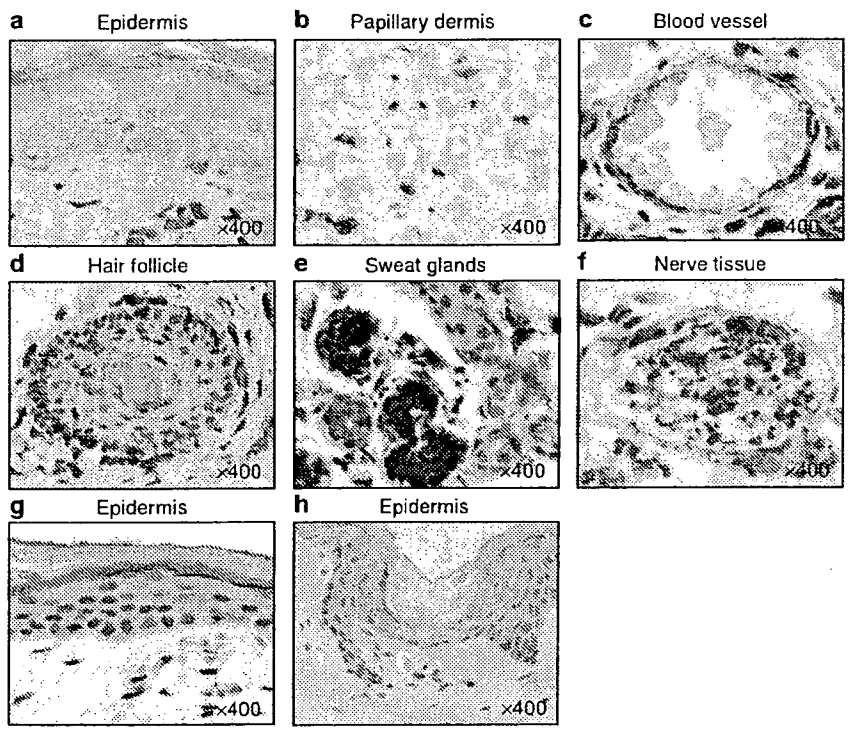

Figure 1. Expression of CXCL12 in normal human skin. Immunohistochemistry staining results using a monoclonal antibody against the chemokine CXCL12 on human normal skin section. (**a**) Stained cells in the basal layer of the epidermis. (**b**) Scattered cells stained in the papillary dermis. (**c**) Endothelial cells and pericytes stained in blood vessel. (**d**) Fibrous sheet stained in the hair follicle. (**e**) Sweat glands not uniformly stained. (**f**) Axons and blood vessels stained in nerve tissue. (**g**) Sections of epidermis and papillary dermis were stained without the primary antibody ensuring that no background staining was received from the second antibody. (**h**) Sections of epidermis and papillary dermis were stained with the primary antibody after incubation with CXCR4 ligands CXCL12α and CXCL12β ensuring that the staining is specific for CXCL12. (Original magnification × 400).

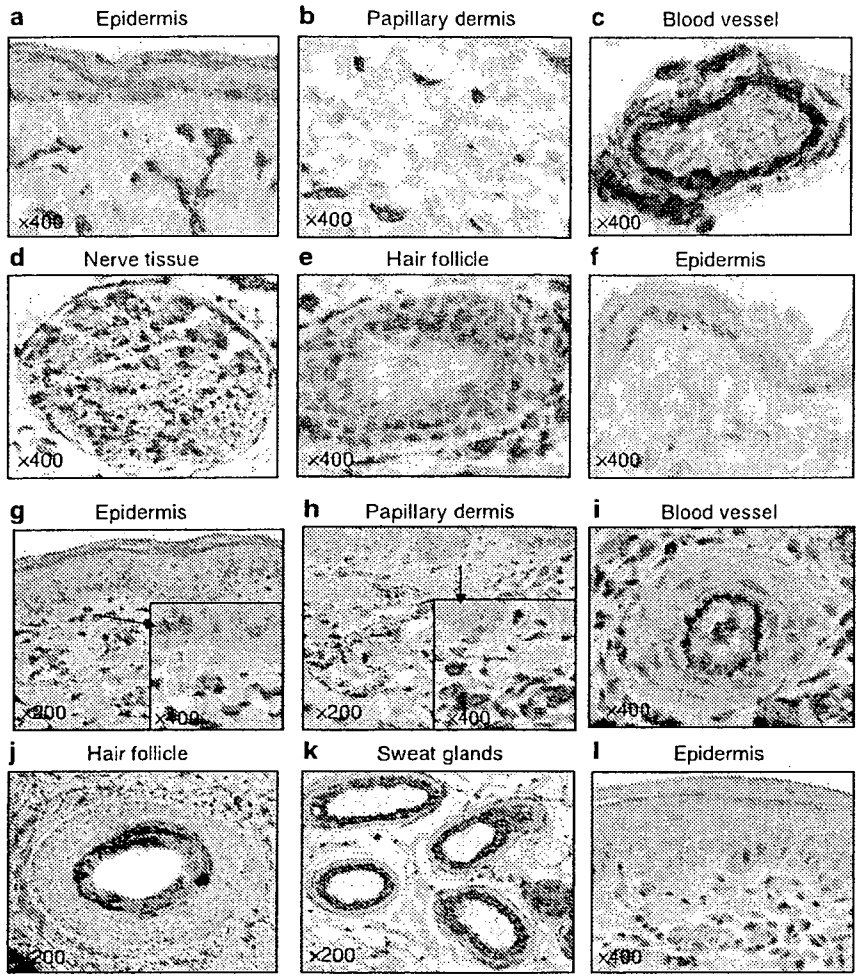

Figure 2. Expression of CXCL12 in rat and swine normal skin. (**a–f**) Immunohistochemical staining results using monoclonal antibody against the chemokine CXCL12 on rat normal skin sections. (**a**) Cells stained in the basal layer of the epidermis. (**b**) Scattered cells stained in the papillary dermis. (**c**) Endothelial cells and pericytes stained in blood vessel. (**d**) Axons and blood vessels stained in nerve tissue. (**e**) Fibrous sheet stained in the hair follicle. (**f**) Epidermis and papillary dermis control staining, without the primary antibody (original magnification of × 400). (**g–l**) Immunohistochemical staining results using monoclonal antibody against the chemokine CXCL12 on swine normal skin sections. (**g**) Cells stained in the basal layer of the epidermis and the papillary dermis. (**h**) Scattered cells stained in the papillary dermis. (**i**) Endothelial cells and pericytes stained in blood vessel. (**j**) Fibrous sheet stained in the hair follicle. (**k**) Sweat glands staining. (**l**) control staining, without the primary antibody. (Original magnifications × 200 or × 400).

chemokine CXCL12 was similarly expressed by swine normal skin cells in the basal layer of the epidermis (Figure 2g), by scattered cells in the papillary dermis (Figure 2h), in pericytes, and by the endothelial layer of blood vessels (Figure 2i). The chemokine CXCL12 was also expressed by fibrous sheets of hair follicles (Figure 2j) and by sweat glands (Figure 2k). No staining was detected with control antibody used to stain the same skin sections (Figure 2l). This unique and conserved expression pattern of CXCL12 may suggest a role for CXCR4/CXCL12 axis in the organization of skin tissue.

Following burns, the level of CXCL12 was markedly increased in human burn blister fluids, hair follicles, blood vessels endothelium, and fibroblasts in the recovering dermis of rat, swine, and human skin.

In order to study the effect of burn injury on CXCL12 expression in the skin, we first collected burn wound fluids, and CXCL12 levels were measured by ELISA assay and compared to the levels of IL-8 (Figure 3a and b). The results indicate a unique pattern of the chemokine CXCL12 expression compared to the IL-8. IL-8 appeared first in the burn fluid a few hours after injury, reached a plateau level after 1 day, and remained at the same level for the next 4 days. CXCL12 appeared a few hours after injury, reached a plateau level after 1 day, and remained at the same level for an additional 2 days, and then the level of CXCL12 decreased exponentially. The consistent overexpression of IL-8 in burn wound fluids and skin tissue has also been reported by others (Iocono *et al.*, 2000). These authors suggested that IL-8 has a role in stimulating neutrophils

migration and accelerating the angiogenic process within the burn wound.

The expression of the chemokine CXCL12 following burn infliction was further examined by immunohistochemical staining of rat skin sections. The results shown in Figure 5 indicate accumulation of CXCL12 in the rat burned skin in correlation with time. Six days and 1 day after injury, CXCL12 was not detected in the burned tissue. Three days postburn, CXCL12 was detected in endothelium blood vessels, in the hair follicles, and also in scattered cells accumulated in the dermis. Five and 7 days postburn, a higher expression of the chemokine was detected in blood vessels and in fibroblast-like cells accumulated in the dermis. As was shown before for human normal skin, CXCR4 was detected in normal and proliferating rat epithelial cells and endothelial cells after burn injury (Figure 4). In the dermis of injured skin, CXCR4 expression was also detected in mononuclear cells as well as infiltrating eosinophils.

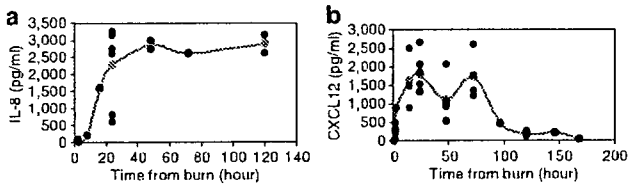

Figure 3. (a) IL-8 and (b) CXCL12 mean levels (pg/ml) in human burn wound fluid collected from blisters of patients with second degree burn. Fluids were collected 0–5 days after burn as a medical treatment protocol. Samples were measured for the chemokines by ELISA assays. Each point represents one patient.

The pattern of CXCL12 expression in swine skin postburn is similar. Four days postburn, CXCL12 was present in endothelium blood vessels and in scattered cells that accumulated in the papillary dermis. Ten days after injury, a strong expression of the chemokine was detected in blood vessels and in the accumulating fibroblast-like cell population in the papillary dermis of normal skin stained for CXCL12 is shown in Figure 5c.

In order to determine the cell types that expressed high levels of CXCL12, we stained parallel sections from burned skin for vimentin and CXCL12. The majority of fibroblast-like cells were stained for both CXCL12 and vimentin indicating that fibroblasts were expressing CXCL12 in the skin following

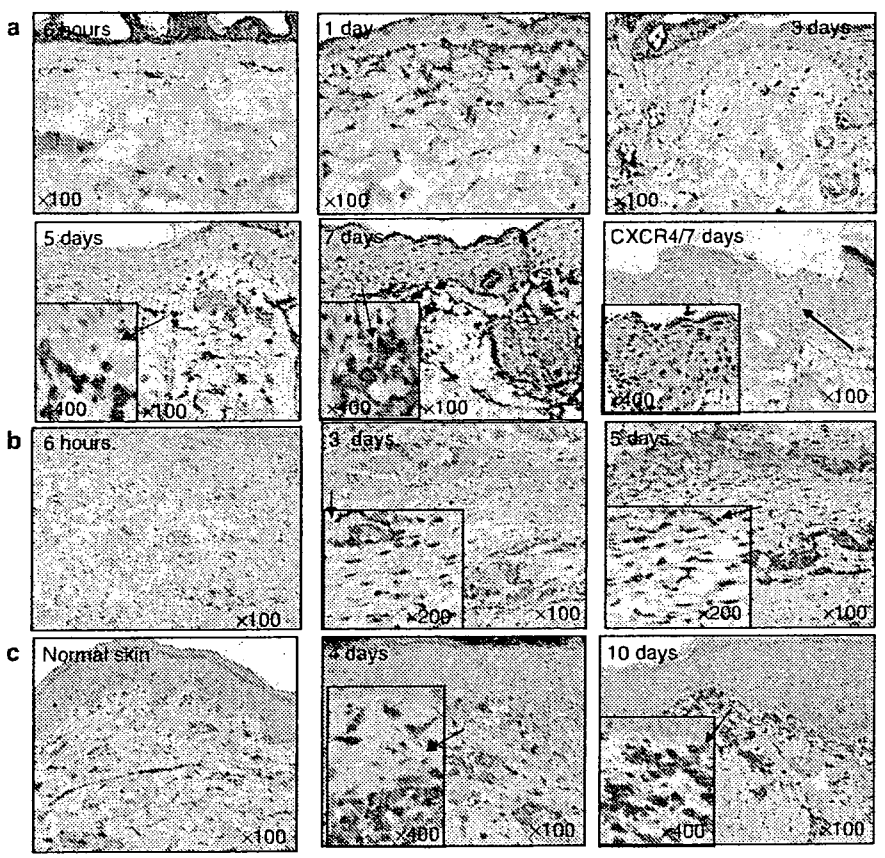

Figure 4. The involvement of CXCL12 in rat and swine burn wound healing. Expression of CXCL12 in rat burn wound healing. (a) Immunohistochemical staining of CXCL12 of rat epidermis burned skin sections, at 6 hours, 1 day, 3 days, 5 days, and 7 days after the burn. Staining for CXCR4 is shown at 7 days after the burn (original magnifications × 100, × 200). (b) Immunohistochemical staining of CXCL12 of rat dermis burned skin sections, at 6, 72, and 120 hours after the burn (original magnifications × 100, × 200). (c) Expression of CXCL12 in swine skin after second-degree burn. Immunohistochemical staining of CXCL12 at 4 days, 10 days after the burn, and at time 0 in normal skin. (Original magnifications × 100, × 400).

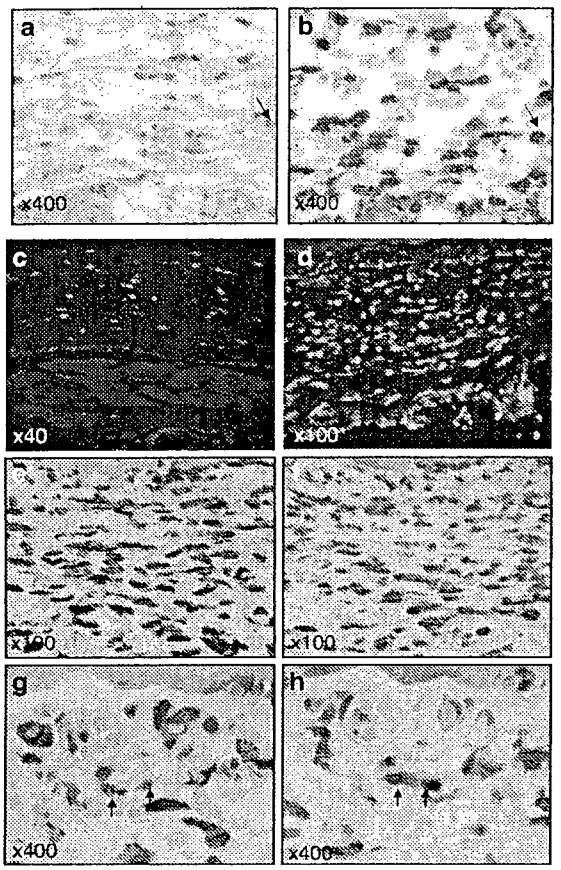

Figure 5. Coexpression of vimentin and CXCL12 in rat burned skin. (**a**) Immunohistochemical staining for vimentin of rat burned skin dermis 5 days after burn. (**b**) CXCL12 immunohistochemical staining of consecutive tissue section of rat burned skin section 5 days after burn (Original magnification × 400; arrow indicates the staining for CXCL12 and vimentin). Coexpression of GPF and CXCL12 in heterozygous mice bearing a GFP reporter knocked-in to the CX3CR1 locus burned skin. (**c** and **d**) Accumulation of GFP + monocyte/dendritic cells in the dermis of injured skin. (**e–h**) Coexpression of GFP + CXCL12 in monocyte/dendritic cells in parallel sections from dermis of injured skin; arrow indicates the staining for CXCL12 and GFP.

burn injury (Figure 5a and b). However, part of the cells that expressed CXCL12 did not express vimentin. CXCL12 was shown to be expressed by human dendritic cells localized to the epidermis and the dermis (Pablos *et al.*, 1999). An excellent means to track monocyte subsets in the skin was through the use of mice bearing a green fluorescent protein (GFP) reporter knocked-in to the CX3CR1 chemokine receptor locus (Qu *et al.*, 2004). Indeed, we found that following injury, monocyte with a dendritic-like shape accumulated in the dermis and epidermis (Figure 5c and d). Part of the monocyte/dendritic cells that expressed the GFP also expressed CXCL12 (Figure 5e–h).

To further study the expression of CXCL12 and CXCR4 in the skin, we used primary skin fibroblast and keratinocyte cultures. In agreement with our *in vivo* results, we found that while the fibroblasts expressed the chemokine CXCL12 in the mRNA level, the keratinocytes did not. In contrast to CXCL12, keratinocytes, but not the fibroblasts, expressed the receptor CXCR4. In order to verify our finding, we used ELISA assay to check the production of CXCL12 by keratinocytes and fibroblasts. The results demonstrated that while keratinocytes did not express the chemokine CXCL12 at the protein level, fibroblasts did express and secrete CXCL12 (Figure 6a), especially during the recovery of skin fibroblasts migrating into the wound area and accumulating in the dermis. In order to study the effect of wounding on CXCL12 expression by skin fibroblasts, a "scratching" assay was performed on confluent layers of human skin fibroblasts *in vitro*. Immunohistochemical staining of confluent human skin fibroblasts showed moderate CXCL12 expression. Two days following scratching, an increase in CXCL12 expression by cells adjacent to the affected area was detected (Figure 6d). Fibroblast monolayers were negatively stained with control antibody against cytokeratin.

Inhibition of the CXCL12/CXCR4 pathway resulted in reduced eosinophil accumulation and improved epithelialization

In order to evaluate the effect of the CXCR4 antagonist, 4F-benzoyl-TN14003, and neutralizing antibodies to the receptor on the recovery of rat skin, we first tested their ability to inhibit the migration of rat lymphocytes in response to CXCL12. Migration assay was carried out on total rat lymphocytes separated by Ficoll gradient, and their migrating ability to medium containing CXCL12 was examined. Lymphocytes were incubated with the CXCR4 antagonist, 4F-benzoyl-TN14003, and an antibody against CXCR4. Treatment of cells with 4F-benzoyl-TN14003 exerted a strong inhibitory effect, whereas treatment of cells with neutralizing antibodies to CXCR4 exerted moderate effect on the migration of cells in response to CXCL12 (Figure 7a).

Next, we examined the inhibitory effect of CXCR4 antagonists on burn wound healing (Figure 7b–d). Inhibitors were injected subcutaneously to the burned area at 0, 1 day, and 3 days, and animals were killed 5 days postburn. Animals injected with the CXCR4 inhibitor, 4F-benzoyl-TN14003, showed an increased epithelialization (Figure 7b). A small but not significant decrease in the polymorphonuclear cell population in the dermis was observed (Figure 7c). However, a strong and significant inhibition in eosinophil accumulation in the dermis was found in the 4F-benzoyl-TN14003 and antibodies to the CXCR4-treated groups (Figure 7d). In contrast to eosinophil accumulation, the accumulation of polymorphonuclear cell population in the epidermis was not affected (Figure 7d). These results suggest a role for CXCR4/CXCL12 interaction in the migration of eosinophils to the skin in the process of epithelialization following burn inflection.

DISCUSSION

Burn wound healing is a complex process consisting of an early phase of energy depletion and necrosis, followed by a two-stage inflammatory phase, formation of granulation tissue, matrix formation, and remodeling (Clark, 1988; Cotran et al., 1999; Spies *et al.*, 2002). The numerous cellular and humoral interactions during these phases of thermal wound healing are complex and not well understood. Partial skin

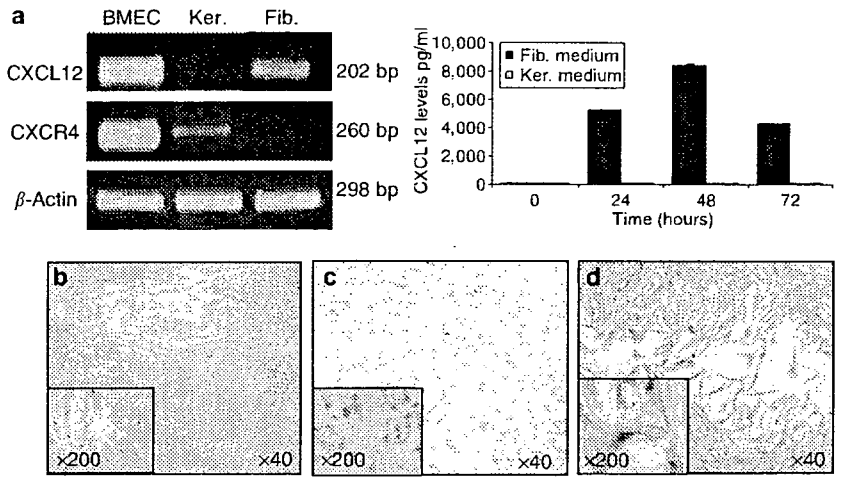

Figure 6. CXCL12 is expressed in primary cultures of fibroblasts, but not in keratinocytes. (a) *In vitro* expression of CXCL12 and CXCR4 in keratinocytes and fibroblasts. Expression of CXCL12 and CXCR4 measured by RT-PCR in primary human keratinocytes and fibroblasts. Expression of CXCL12 in keratinocytes- and fibroblasts-conditioned medium as measured by ELISA assay. (b) Immunostaining of human primary fibroblasts with anti-cytokeratin antibodies as control. (c) Immunostaining of human primary fibroblasts with anti CXCL12 antibodies. (d) Immunostaining of human primary fibroblasts with anti-CXCL12 of human primary fibroblast 2 days after wounding the fibroblasts monolayer. (Original magnifications × 40 and × 200). Fib.=fibroblasts; Ker.=keratin.

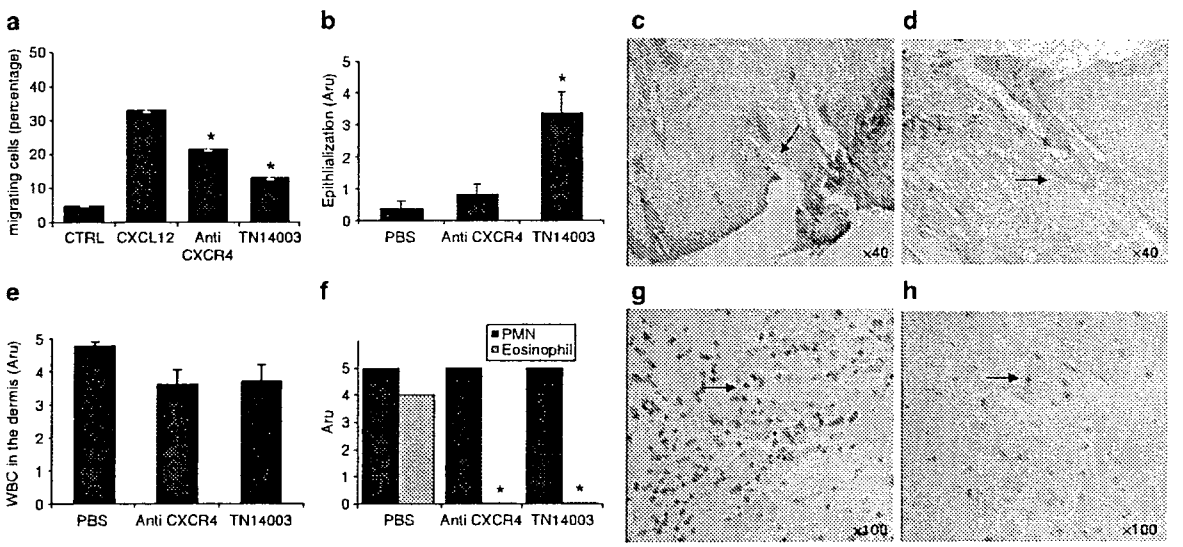

Figure 7. Effect of neutralizing antibodies to CXCR4 and the small peptide inhibitor of CXCR4 on inflammation and regeneration of skin following burns. (a) Migration of rat lymphocytes in response to CXCL12 (100 ng/ml) was tested in the absence and presence of neutralizing antibodies to CXCR4 (NA), or the CXCR4 antagonist – 4F-benzoyl-TN14003. (b) The effect of CXCR4 antagonists on re-epithelialization. (c) Depicts the epithelialization of burned skin in mice treated with phosphate-buffered saline (PBS) (asterisk indicates the sites of novel epithelialization). (d) Depicts the epithelialization of burned skin in mice treated with 4F-benzoyl-TN14003 (asterisk indicates the sites of novel epithelialization). The number of lymphocytes in the dermis is shown in (e). The number of polymorponuclear cells (PMN) in the epidermis and eosinophils in the dermis 5 days after burn is shown in (f). (g) Depicts the eosinophils in the dermis of mice treated with PBS (arrow indicates the site of eosinophilia). (h) Depicts the eosinophils in the dermis of mice treated with 4F-benzoyl-TN14003 (arrow indicates the site of eosinophilia). The results are the average of two experiments; for each experiment at least five rats were tested ($P<0.05$).

burn wounds could be more effectively treated sooner if the blister wall was maintained intact (Ono *et al.*, 1995). Burn wound fluids from blisters contain relatively large amounts of cytokines such as platelet-derived growth factor, IL-6, transforming growth factor-β, and IL-8 thought to stimulate the wound healing process by regulating epithelialization (Ono *et al.*, 1995; Struzyna *et al.*, 1995). The increased CXCL12 levels in human burn fluid during the first 3 days following burn injury (Figure 3b) and the expression of CXCR4 by human keratinocytes (Figure 4a) may support the survival and tissue organization of these cells. This concept is supported by studies showing that CXCR4 is expressed by

skin keratinocytes and is essential for keratinocytes that participate in maintaining skin integrity (Smith *et al.*, 2004). The restricted presence of functional CXCL12 (24–48 hours following burn) may suggest a protective role for CXCL12 in the maintenance of skin tissue following burn. In contrast to the presence of CXCL12 in human burn fluid during the first 3 days following injury, an increased number of fibroblasts and dendritic cells that expressed CXCL12 are observed in the regenerating skin in the first 2 weeks following damage. This difference may be the result of increased levels of proteolytic activity in the burn fluid. Indeed, a variety of proteolytic enzymes such as cathepsin G, elastase, and matric metalloproteinase-9 were recently shown to degrade CXCL12 (Petit *et al.*, 2002).

In partial-thickness burns, the epidermis and the superficial dermis are destroyed and undergo necrosis (Clark, 1988; Cotran *et al.*, 1999; Singer and Clark, 1999). Twenty-four hours to 2 days following burns, the affected area lost CXCL12 expression. However, the expression of CXCL12 in the area adjacent to the burn wound was intensed. During this time period, a massive influx of neutrophils into the wound area was observed. The accumulation of neutrophils could not be blocked by CXCR4 antagonists, suggesting that CXCR4/CXCL12 axes have no detectable role in this process. The accumulation of neutrophils in the wound area was associated with an increased production of the neutrophil chemoattractants neutrophil activating protein-2 (NAP-2), Growth-Regulated Oncogene alpha (GRO-α), and Epithelial neutrophil activating peptide-78 (ENA-78), as well as with the sustained production of IL-8 in human burn blisters in human (Figure 3a) (Faunce *et al.*, 1999; Piccolo *et al.*, 1999; Gillitzer and Goebeler, 2001). In partial-thickness burns, the proliferating and migrating epithelium arose from the wound border as well as from hair follicles. The rate of epithelial cover was modulated by growth factors that stimulated the proliferation and chemotaxsis of epithelial cells (Clark, 1988; Cotran *et al.*, 1999; Singer and Clark, 1999). During the granulation phase, beginning 2–3 days following damage, fibroblasts attracted by macrophages migrated into the wound area; these fibroblasts from swine and rat origin secreted high levels of CXCL12 (Figures 4 and 5). The process of granulation is associated with intense angiogenesis (Cotran *et al.*, 1999; Singer and Clark, 1999). In parallel to migration of fibroblasts expressing high levels of CXCL12, novel and resident endothelial cells lining the blood vessels also expressed CXCL12. During this phase of wound healing, a second wave of immune cells entered the epidermis underlying the burn. These cells include macrophages, lymphocytes, and eosinophils. The chemokines CCL2, CXCL10, CXCL9, and CCL22 were found to be spatially associated with lymphocyte and monocyte accumulation (Gibran *et al.*, 1997; Gillitzer and Goebeler, 2001). We found a minor effect of CXCR4 antagonists on the recruitment of macrophages and lymphocytes, whereas the recruitment of eosinophils was totally blocked (Figure 7).

A fine balance between fibrotic tissue deposition and neovascularization on the one hand and fibrotic tissue degradation and epithelization on the other should be maintained in order to assure successful wound healing. Immune cell subpopulation recruited to the burned site is involved in orchestrating these events. Unbalanced proliferation and activation of fibroblasts may lead to inadequate granulation and the formation of a fibrotic tissue. However, reduced angiogenesis and blood flow into the burn wound can prevent successful epithelialization and wound repair. With regard to the CXCL12/CXCR4 axis, we have found that the most dramatic effect of CXCR4 antagonists was on the number of infiltrating eosinophils. The decrease in eosinophil migration into the wounded tissue and the increased epithelialization observed in mice treated with CXCR4 antagonist indicate that CXCL12/CXCR4 interactions are involved in shaping the balance between fibrosis and epithelialization. Moreover, these data may suggest that eosinophils are linked to the regulation of epithelialization.

Indeed, it was reported by Yang *et al.* (1997) that anti-interleukin-5 mAB (TRFK-5) treatment can deplete eosinophils in healing of cutaneous wounds and that wound closure by re-epithelialization in the treated animals was 4 days faster than in the control group. This study suggests a role for eosinophils in negatively affecting wound re-epithelialization. Neutralizing antibodies to CXCR4 and AMD3100, an antagonist of CXCR4/CXCL12 interaction, were shown to reduce lung eosinophilia, indicating that CXCR4-mediated signals contribute to lung inflammation in a mouse model of allergic airway disease (Gonzalo *et al.*, 2000; Lukacs *et al.*, 2002). Eosinophils constitutively express CC chemokine receptor 3 and, to a lesser extent, CC chemokine receptor 1. CC chemokine receptor 3 is mainly responsible for migration of resting eosinophils, and its specific ligand, eotaxin, represents the most potent chemoattractant for eosinophils (Nagase *et al.*, 2001b). However, eosinophils in inflamed tissue sites exhibited a decreased CC chemokine receptor 3 and an increased CXCR4 expression (Nagase *et al.*, 2001a). Surface CXCR4 protein was hardly detectable in the peripheral blood or freshly isolated eosinophils. Similarly to the phenomenon observed with eosinophils in inflamed tissues, surface expression of CXCR4 became gradually apparent during *in vitro* incubation of cells. CXCL12, the natural ligand of CXCR4, elicited an apparent Ca^{2+} influx in these cells and induced a strong migratory response comparable to that by eotaxin (Nagase *et al.*, 2000)

In summary, we suggest that the presence of CXCL12 in burn blisters is involved in protecting the skin during a short period of time following skin burn injury. Thereafter, CXCL12 expressed by fibroblasts and endothelial cells may induce the accumulation of eosinophils, which in turn slow the epithelialization. Our data suggest that CXCL12 is more predominantly supporting fibrosis than epithelialization. Indeed, we and others have recently shown that during liver fibrosis, the levels of CXCL12 expression by endothelial cells and fibroblasts are dramatically increased (Wald *et al.*, 2004). It is therefore possible that by using inhibitors against CXCR4, the balance between fibrosis and epithelialization can be changed, thereby leading to a better and faster recovery of skin following damage.